Semiclassical and quantum polarons in crystalline acetanilide

P. Hamm[1,a] and G.P. Tsironis[2,3,b]

[1] Physikalisch-Chemishes Institut, Universität Zürich, Winterhurerstr. 190, 8057, Zürich, Switzerland
[2] Department d' Estructura i Constituents de la Matéria, Facultat de Física, Universitat de Barcelona, Diagonal 647, 08028 Barcelona, Spain
[3] Department of Physics, University of Crete and Institute of Electronic Structure and Laser, FORTH, PO Box 2208, Heraklion 71003, Crete, Greece

Abstract. Crystalline acetanilide is a an organic solid with peptide bond structure similar to that of proteins. Two states appear in the amide I spectral region having drastically different properties: one is strongly temperature dependent and disappears at high temperatures while the other is stable at all temperatures. Experimental and theoretical work over the past twenty five years has assigned the former to a selftrapped state while the latter to an extended free exciton state. In this article we review the experimental and theoretical developments on acetanilide paying particular attention to issues that are still pending. Although the interpretation of the states is experimentally sound, we find that specific theoretical comprehension is still lacking. Among the issues that that appear not well understood is the effective dimensionality of the selftrapped polaron and free exciton states.

1 Introduction

The first numerical experiment performed by Fermi, Pasta and Ulam in 1955 proved to be the beginning of an exciting, non-reductionist branch of modern science focusing on nonlinearity and complexity in a variety of physical systems [1]. In this path, the discovery of the soliton in the sixties by Zabusky and Kruskal and the understanding of many of its mathematical properties led in the seventies in the exploration for physical applications. Proposals for soliton modes in Josephson junctions, optical fibers and other physical systems where suggested at this time, while Davydov introduced the novel idea that solitons may have a direct impact to biology as well [3–5]. More specifically Davydov proposed that the energy released in the process of ATP hydrolysis becomes vibrationally selftrapped and forms a soliton. The main feature that made solitons appealing to biology is their property of dispersiveless transport; if a soliton-like packet of energy forms in a macromolecule, it may propagate without losses and enable long range coherent energy transfer. This feature could be critical in the internal energetics of proteins where energy deposited on given sites produces large effects at relatively distant locations. Although soliton propagation experiments in proteins were not possible at this time, Careri and coworkers were investigating independently crystalline acetanilide (ACN), a molecular solid that has peptide bonds and a structure similar to that of a protein [6] (figure 1). They found in infrared absorption experiments that an "anomaly" appears in the amide-I spectral region manifested through a strongly temperature dependent spectral peak

[a] e-mail: phamm@pci.unizh.ch
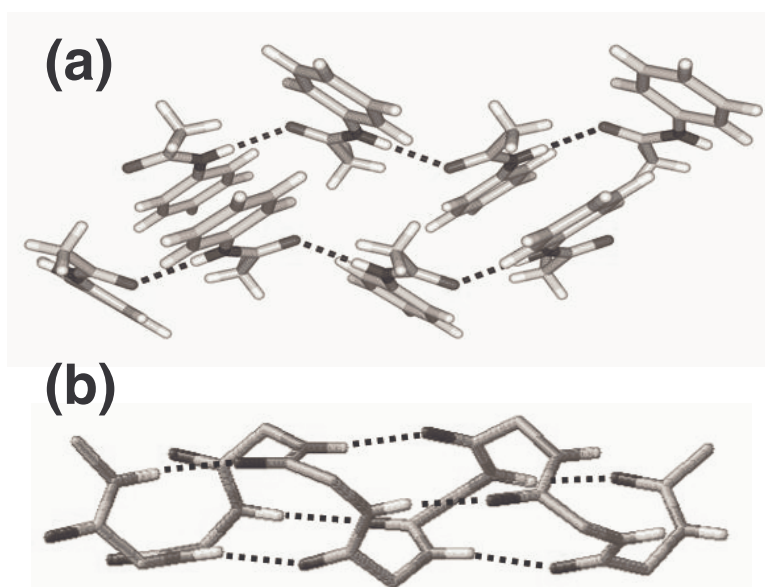[b] e-mail: gts@physics.uoc.gr

Fig. 1. Comparison of (a) crystalline acetanilide; dots denote the two hydrogen bond chains formed, and (b) an α-helix that is part of a polypeptide. The α-helix forms three hydrogen bond chains.

[7,8] (figure 2). In the early eighties Scott and collaborators surmised that this peak was related to a Davydov soliton [7,9,10]. Davydov's original soliton idea coupled to the experimental findings of Careri and theoretical picture of Scott for ACN lead to a furry of activity during the rest of the decade as well as in the early nineties. Brown et al. examined critically the general "Davydov soliton" hypothesis [11,12] while in acetanilide Scott as well Alexander and Krumhansl soon realized that it was a small polaron rather than an extended soliton responsible for the anomalous peak [10], [13–15]. The small polaron picture corroborated the neutron and absorption experiments of Barthes and collaborators [16,17]. During the same period, explicit lattice discreteness was introduced in nonlinear approaches and, as a result, a new entity was introduced, viz. that of an intrinsic localized mode or discrete breather [18]. The latter modes where seen in many instances to describe better nonlinear localization than continuous solitons. The over thirty-year long history of the fertile Davydov soliton idea is landmarked presently by a new generation of experiments; the pump-probe experiments of Hamm and collaborators have not only corroborated the acetanilide picture but also produced the first experimental sign for nonlinearly localized states in proteins [19–22]. In the present work we will attempt to summarize the basic theoretical and experimental steps in the Davydov soliton idea as related specifically to acetanilide. We prefer to focus only on the latter since the excellent review by Scott in 1992 covers much of the generalities on the theoretical Davydov soliton idea, while,additionally, acetanilide provides a tangible system where both theory and experiments have been employed.

Nonlinear excitations in biomolecules are typically associated with with objects such as solitons, polarons or discrete breathers (DBs). All three modes are similar in nature in that they arise due to the actual or effective presence of some type of nonlinearity in the equations of motion. In the original formulation of the Davydov problem, a vibrational excitation (a C=O stretching quantum, or a $C = O$ exciton or a vibron) with typical energy of about 1665 cm^{-1} is coupled to lattice phonons with energies that are more than one order of magnitude smaller. Due to the assumed strong exciton-phonon coupling, the bear exciton becomes self-trapped and forms a polaron, i.e. a new entity that is localized and has lower overall energy than the extended exciton. Depending on the relative values of the exciton hopping term, the phonon frequency and the exciton-phonon coupling one may arrive to a polaron that is small, i.e. localized to essentially on one site, large, i.e. much larger than few sites, as well as having distinct intermediate features depending on the parameters. The Davydov soliton is a special
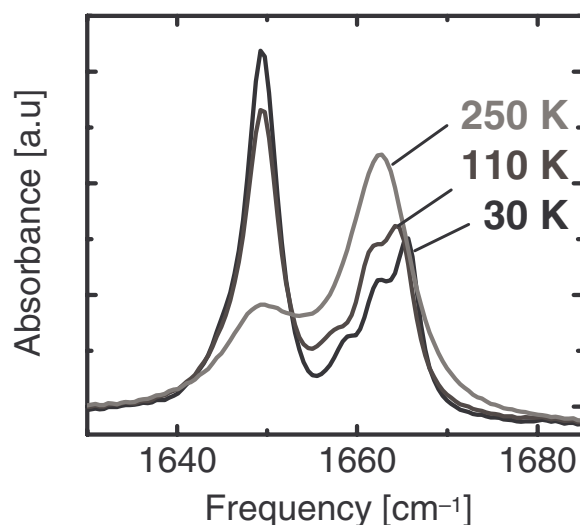
Fig. 2. IR spectroscopy of acetanilide. The "normal" and the "anomalous" peak.

kind of large polaron that is formed when phonons respond in an organized, coherent way to the presence of the exciton. Both the large polaron and the Davydov soliton are approximate, semi-classical solutions since their creation involves a large number of phonons; they are described mathematically through the celebrated Nonlinear Schrödinger Equation (NLS), an integrable nonlinear partial differential equation [2,23]. Discrete breathers, on the other hand, are localized solutions of discrete nonlinear equations and differ substantially from the extended solitons or large polarons. They involve a local lattice oscillation that is stable due to the disparity of its frequency to the linearized frequency modes of the lattice. Although polarons, solitons and DB's are in many ways related, especially in some limits, it is useful to differentiate among them in order to obtain a clearer understanding of the problem. An important mathematical difference between polarons on one hand and solitons or DB's on the other is that the former appear in coupled systems involving two fields, e.g. excitons coupled to phonons, whereas the latter are typically single field nonlinear equation solutions. In the latter the second field has been eliminated through an approximate procedure and replaced by an effective nonlinear term acting explicitly on the degree of freedom of interest.

In this review will attempt to describe the various theoretical approaches used in the analysis of the acetanilide study and related them to the different experiments. We will start (section 2) with a brief description of the original infrared absorption experiment of Careri et al. that linked for the first time the anomalous amide-I band to a selftrapped state. In order to proceed with the theoretical analysis we will introduce the Holstein Hamiltonian and focus first on a semiclassical treatment (section 3). This will enable us to describe the standard adiabatic-like polaron acetanilide picture as provided by Scott [10]. Subsequently (section 4) we focus on a fully quantum mechanical approximate analytical approach that will give further insight on the acetanilide polaron. In section 5 we discuss the issue of the free exciton as appears in the semiclassical as well as the approximate quantum mechanical treatments. Subsequently (section 6) we discuss exact numerical solutions of the quantum problem and point out similarities as well as differences to the semiclassical solutions. In section 7 we present the pump-probe experimental results and compare them to the exact numerics. Finally in section 8 we summarize this work and conclude.

2 The acetanilide story

2.1 Acetanilide and the early experiments

Crystalline acetanilide $(CH_3\text{-}COONH\text{-}C_6H_5)_n$ is an organic molecular crystal that forms two close hydrogen-bonded chains running along the b direction of the lattice (figure 1). The

nearly planar amide groups have bond distances comparable to those in polypeptides and, as a result, it may be studied instead of more complex protein and still provide useful polypeptide dynamical information. The infrared absorption spectrum shown in figure 2 shows two main peaks in the amide-I spectral region; a strongly temperature dependent line at approximately $1650\,\mathrm{cm}^{-1}$ as well as basically temperature independent one at $1665\,\mathrm{cm}^{-1}$ [7,8]. While the "normal" $1665\,\mathrm{cm}^{-1}$ peak was assigned to one quantum of a C=O vibration of an acetanilide hydrogen bonded chain, the origin of the anomalous band was not so clear and could be a signature of a Fermi resonance or some structural transition. Both these possibilities were ruled out by Careri et al. favoring a then "unconventional" explanation that related the band to a "Davydov-like soliton" arising through coupling of the amide exciton to phonon modes [7]. Careri, Scott and collaborators used experimental indications and assumed that the C=O excitation is coupled to an optical stretching mode of the hydrogen bond connecting carbon and nitrogen atoms within the peptide group [8,9]. Absence of involvement of acoustic modes in the C=O selftrapping was indicated later through neutron scattering experiments by Barthes et al. [24]. The theoretical picture that the anomalous band is due to a dynamically localized selftrapped state permit the quantitative explanation of the line temperature dependence using the physics of color centers [25]. The experimental and theoretical picture that emerged in the late eighties asigning the anomalous spectral line to a small Holstein-like polaron has been corroborated by the recent experiments of Hamm et al. [19–22] that will be reviewed in more detail later. A brief historical exposition of the acetanilide developments is given in the appendix I.

2.2 The Holstein Hamiltonian

Davydov's molecular soliton model involves the coupling of a vibrational exciton to acoustic phonons. The interaction of the excitation with phonons, modifies the latter that in-turn affect the former in a selfconsistent way, leading, under several approximations, to an NLS-like soliton [3–5], [23]. In the case of acetanilide, the initial indications were that the phonons responsible for selftrapping were optical in the frequency range $20\,\mathrm{cm}^{-1} \leq \omega \leq 100\,\mathrm{cm}^{-1}$; as a result, Careri et al. used the Holstein Hamiltonian instead of the Davydov one. While the theoretical work of Alexander and Krumhansl [14] used coupling to acoustic phonons, subsequent experimental work by Barthes did not indicate a strong presence of an acoustic branch in the low ACN IR spectrum [16,17], [24]. Additionally, recent pump-probe experiments seem to show that a unique phonon of frequency approximately equal to $\omega = 50\,\mathrm{cm}^{-1}$ is responsible for the selftrapping phenomenon [19]. Although one may not consider the absence of an acoustic branch or even an optical branch with dispersion as a closed issue, we may, following the overwhelming number of approaches, make the assumption that the physics of the amide-I lines may be described by the following Holstein Hamiltonian [26]:

$$H = H_{ex} + H_{ph} + H_{int} \tag{1}$$

$$H_{ex} = \hbar\Omega \sum_{j=1}^{N} (B_J^\dagger B_j + 1/2) - J \sum_{j=1}^{N} (B_j^\dagger B_{j+1} + B_j^\dagger B_{j-1}) \tag{2}$$

$$H_{ph} = \hbar\omega \sum_{j=1}^{N} (b_j^\dagger b_j + 1/2) \tag{3}$$

$$H_{int} = \chi \sum_{j=1}^{N} B_j^\dagger B_j (b_j^\dagger + b_j) \tag{4}$$

with

$$b_j = \frac{1}{\sqrt{2}} \left(\sqrt{\frac{m\omega}{\hbar}} q_j + \frac{i}{\sqrt{\hbar m\omega}} p_j \right) \tag{5}$$

$$b_j{}^\dagger = \frac{1}{\sqrt{2}} \left(\sqrt{\frac{m\omega}{\hbar}} q_j - \frac{i}{\sqrt{\hbar m\omega}} p_j \right) \tag{6}$$

where $B_j^\dagger$ (B_j) creates (annihilates) a C=O vibron at site j (of N sites in total), q_j, p_j are the position and momentum of the j-th optical oscillator respectively while $b^\dagger{}_j$, b_j are the corresponding phonon creation and annihilation operators. In equations (1)–(4) $\hbar\omega$ is the energy of the bare amide-I exciton equal to $\hbar\Omega \approx 1565\,\mathrm{cm}^{-1}$ while, the optical phonon energy is, as noted previously, $\hbar\omega \approx 50\,\mathrm{cm}^{-1}$. The exciton nearest neighbor overlap is of the order $J \approx 5\,\mathrm{cm}^{-1}$ while exciton-phonon coupling is $\chi \approx 25\,\mathrm{cm}^{-1}$. We note that acetanilide presents a unique problem in molecular crystals were the three parameters entering in the Hamiltonian, viz. J, χ and ω are known to reasonable confidence.

The C=O dipole-dipole interaction transfer integral is very small in acetanilide, and thus, the bear exciton band is very narrow and the exciton is immobile. Since the phonon frequency ω is much larger than J, phonons react very fast to the slow excitons that tunnel from site to site; the phonons then follow adiabatically the slowly tunneling exciton motion. Finally, since the exciton-phonon coupling χ is relatively large compared to J, one expects that a small, very localized polaron may form that is not very mobile. In order to treat the ACN parameter regime in the Holstein model we must resort in principle to a fully quantum mechanical treatment since we are in the regime where the phonon frequency is much larger than the exciton transfer J. Since the first treatment was done through the Davydov ansatz, we will first resort to semi-classics and subsequently investigate the connection of this approach with the fully quantum mechanical one.

3 Semiclassical Holstein polaron in one dimension

3.1 Classical phonon approach

When either J or χ are large many phonons are excited and the zero point quantum motion is not important; in these cases we may use the semiclassical limit and treat phonons classically [27]. In many practical cases, the excitation of even few phonons is sufficient for rendering the modes classical. Under this assumption, while the excitons retain their full quantum nature, the phonon operators $b_j^\dagger$ and b_j become c-numbers denoted by b_j^* and b_j, respectively. Furthermore, if in this multiple phonon regime, the atomic motion becomes more sluggish, then we may consider the now classical phonons as "slow", leading to $p_j \approx 0$, i.e $b_j^* \approx b_j$, i.e. b_j is real. With these assumptions, the semiclassical Hamiltonian reads

$$H_{ex} = \sum_{j=1}^{N} \left[\hbar\Omega B_j^\dagger B_j - J(B_j^\dagger B_{j+1} + B_j^\dagger B_{j-1}) + \hbar\omega b_j^* b_j + \chi B_j^\dagger B_j(b_j^* + b_j) \right]. \tag{7}$$

In order to apply a variational procedure we need first to express the Hamiltonian operator in a specific representation, since otherwise operators would have to be equated with c-numbers. Using the one-exciton state

$$|\psi\rangle = \sum_{j=1}^{N} \psi_j B_j^\dagger |0\rangle_{ex} \tag{8}$$

we obtain the expected value of the Hamiltonian of equation (7) with respect to the state of equation (8):

$$H_{sc} = \langle\psi|H_{ex}|\psi\rangle = \sum_{j=1}^{N} \left[\hbar\Omega|\psi_j|^2 - J(\psi_j^*\psi_{j+1} + \psi_j^*\psi_{j-1}) + \hbar\omega b_j^* b_j + \chi|\psi_j|^2(b_j^* + b_j) \right]. \tag{9}$$

Variational minimization of equation (9) with respect to the b_j^*, gives

$$b_j = -\chi|\psi_j|^2 \tag{10}$$

leading, after substitution to the Hamiltonian (9) to

$$H_{sc} = \sum_{j=1}^{N} \left[\hbar\Omega|\psi_j|^2 - J(\psi_j^*\psi_{j+1} + \psi_j^*\psi_{j-1}) - \frac{\chi^2}{\hbar\omega}|\psi_j|^4 \right]. \tag{11}$$

Use of Hamilton's equations of motion for the variables ψ_j and $i\psi_j^*$ results in the dynamical equation

$$i\hbar\dot{\psi_j} = \hbar\Omega\psi_j - J(\psi_{j+1} + \psi_{j-1}) - \frac{2\chi^2}{\hbar\omega}|\psi_j|^2\psi. \tag{12}$$

This is the celebrated Discrete Selftrapping Equation (DST) or Discrete Nonlinear Schrödinger Equation (DNLS) [27,28]. It is a semiclassical equation for the vibrational exciton of an amide-I mode obtained after the complete elimination of the phonon degrees of freedom; it provides an approximate description for the dynamics of the exciton when coupled to phonons.

Within the classical phonon assumption, it is possible to improve the DNLS approximation of equation (12) by retaining the dynamics of the classical phonon modes. To this effect, instead of performing the variational minimization to equation (8), we may use Hamilton's equations with respect to phonons and obtain a coupled set of two equations, one for the exciton amplitudes and the second for the classical phonons [27]. The resulting set is compatible with the Born-Oppenheimer approximation:

$$i\hbar\gamma\frac{d\psi_j}{d\tau} = -(\psi_{j+1} + \psi_{j-1}) + \alpha\psi_j u_j \tag{13}$$

$$\frac{d^2 u_j}{d\tau^2} + u_j = -\alpha|\psi_j|^2 \tag{14}$$

where u_j a dimensionless displacement with $\tau = \omega t$, $\alpha = \chi\sqrt{2/\hbar\omega J}$ and $\gamma = \hbar\omega/J$ [27]. The parameter γ controls the relative time scales of phonons compared to J. For stationary phonon displacements we recover the DNLS equation; this may also accomplished in the limit $\gamma \to 0$.

3.2 Coherent state treatment

It is instructive to use an alternative approach based on coherent states in order to investigate the semiclassical limit of the Holstein Hamiltonian. We now make no assumption on the nature of the phonons but assume that the latter are distributed in coherent states, viz. the individual quantum vibrational oscillators are displaced. As a result, we use instead of the state of equation (8) the following:

$$|\psi\rangle = \sum_{j=1}^{N} \psi_j B_j^{\dagger}|0\rangle_{ex}|\phi_j\rangle \tag{15}$$

$$|\phi_j\rangle = e^{\phi_j b_j^{\dagger} - \phi_j^* b_j}|0\rangle \tag{16}$$

where ϕ_j, ϕ_j^* are the complex coefficients that characterize the coherent state at the j-th oscillator and $|0\rangle$ is the phonon vacuum. Application of state of equation (15) to the Hamiltonian (1-4), and ignoring the constant terms arising from the zero point motions leads:

$$H_{sc}' = \sum_{j=1}^{N} \left[\hbar\Omega|\psi_j|^2 - J(\psi_j^*\psi_{j+1} + \psi_j^*\psi_{j-1}) + \hbar\omega|\phi_j|^2 + \chi|\psi_j|^2(\phi_j + \phi_j^*) \right]. \tag{17}$$

Variational minimization of equation (17) with respect to ϕ_j^* gives the condition

$$\phi_j = -\frac{\chi}{\hbar\omega}|\psi_j|^2 \tag{18}$$

that, upon substitution to equation (17) results in the semiclassical Hamiltonian of equation (11). In other words this method leads to the same DNLS equation (12), as the classical phonon approach. Furthermore, treating $\phi, i\phi^*$, as conjugate dynamical variables and applying Hamilton's equations to the Hamiltonian of equation (17) results straightforwardly in the equations of motion (13, 14).

We observe that both methods used, viz. the one that treats the phonons directly as classical and the other that is fully quantum mechanical but assumes the phonons are in local coherent states, lead to *identical* dynamical equations for the excitons. These are the DNLS equation, when the phonons are completely eliminated, or the coupled set of equations (13, 14) in the Born-Oppenheimer approximation. As a result, the variational coherent state method is simply an equivalent but different way of performing the semiclassical approximation.

3.3 Acetanilide analysis

The semiclassical equations (12) as well as (13, 14) may be used for the analysis of the acetanilide problem. We follow Careri et al. [8] and observe that DNLS equation of (12) has two types of solutions: (i) In the limit $N \to \infty$ the extended, free exciton solution $\psi_j = 1/\sqrt{N}e^{-i(kan-Et)/\hbar}$ with energy E, wavevector k and where a is the lattice spacing. The energy of this solution is

$$E_{ex}(k) = \hbar\Omega - 2J\cos(ka) \tag{19}$$

where k is the wavevector and a the lattice spacing. The extended solution describes a band of Bloch wave excitons with very small dispersion and bandwidth $4J$; the lowest energy state is that of the $|k = 0\rangle$ exciton state, the one that is typically excited in spectroscopy with energy $E_{ex} = E(k = 0) = \hbar\Omega - 2J$. (ii) The selftrapped solution where the probability amplitude ψ_j is centered at a given lattice site and decays exponentially around that site. The selftrapped state may be constructed numerically through an iterative procedure starting from the anticontinuous limit at zero coupling, i.e for $J = 0$; it corresponds to a simple discrete breather of the DNLS equation [27]. To lowest order the selftrapped state energy is calculated by substituting $\psi_j = \exp(-iE_{pb}t/\hbar)$ and ignoring the inter-site coupling J that is small; we obtain $E_{pb} = \hbar\Omega - \chi^2/\hbar\omega$. The binding energy then of the selftrapped solution, i.e the total excitonic energy gain of the selftrapped solution with respect to the free exciton solution is

$$E_b = E_{ex} - E_{pb} \approx -\frac{\chi^2}{\hbar\omega} + 2J. \tag{20}$$

This is approximately the amount of energy one gains by forming a localized state in one dimension compared to the extended, long wavelength Bloch state.

According the interpretation of Careri et al. [8,10], the temperature dependent peak of acetanilide corresponds to the selftrapped state, the peak at $1665\,\mathrm{cm}^{-1}$ is the free exciton, while the difference in energy between the two peaks gives the selftrapped state binding energy. We note that the selftrapped state is a small semiclassical Holstein polaron described trough the DNLS equation; as a result we may also call it a discrete breather [27]. As expected, this is a fully localized state that can only acquire band character if the eliminated quantum fluctuations are put back in the picture. The semiclassical picture for the IR absorption experiments of the amide-I mode assumes that only one optical phonon mode of energy $\hbar\omega \approx 50\,\mathrm{cm}^{-1}$ participates the process; this leads in the adoption of the Holstein model for the description of the physics. Three assumptions are subsequently made, viz. (i) the phenomena may be described by a one-dimensional model due to the quasi-one dimensional nature of the crystal in the direction of the hydrogen bonds. (ii) multiple phonons are excited, and as a result, the phonon variables may be taken to be classical and (iii) these classical phonon variables may be very slow. The semiclassical picture then gives a clear physical picture for the two peaks assigning the "anomalous" one to a small polaron selftrapped state and the normal one to a free exciton state.

Although the semiclassical picture is successful in the assignment of the two spectral lines it cannot address the temperature dependence of the anomalous peak; for the latter one needs to
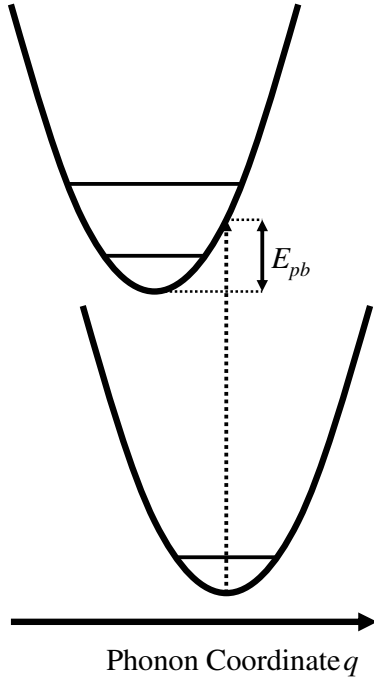
Fig. 3. The displaced oscillator picture; E_{pb} is the exciton energy gain due to coupling to phonons.

consider directly phonon excitations, that nevertheless have been eliminated due to the classical phonon approximation. One way to proceed is by ignoring polaron hoping motion altogether (since J is small) and requantizing the previously assumed classical phonons. We obtain the picture of figure 3 where the two parabolas correspond to phonons around the no-exciton and one-exciton states respectively; the latter state is displaced with respect to the no-exciton state due to the exciton-phonon interaction. In this picture, the polaron line temperature dependence is obtained similarly as in the cases of color centers in molecular solids [25]. It is provided through the sum of all overlaps between equal phonon quanta states of the ground and displaced excited states weighted by the initial (thermal) population of the phonon states, viz. [10]

$$W(T) = \sum_{n=0}^{\infty} P_n |\langle n|\phi_n\rangle|^2 \tag{21}$$

$$P_n = \left[1 - \exp\left(-\frac{\hbar\omega}{k_BT}\right)\right]\exp\left(-n\frac{\hbar\omega}{k_BT}\right) \tag{22}$$

where $|n\rangle$ is ground state with n phonons, $|\phi_n\rangle$ is a displaced oscillator state with equal number of phonons, while P_n gives the equilibrium distribution of phonons at temperature T. The Frank-Condon factor $W(T)$ is found to be [10]:

$$W(T) = \exp\left[-\frac{\chi^2}{\hbar\omega^2}\coth\left(\frac{\hbar\omega}{2k_bT}\right)\right]I_0\left[\frac{\chi^2}{\hbar\omega^2}\mathrm{csch}\left(\frac{\hbar\omega}{2\mathrm{k_b}T}\right)\right] \tag{23}$$

where I_0 is the modified Bessel function of first kind and order zero. It is found that this expression describes correctly the temperature dependence of the anomalous peak [10].

Although the semiclassical picture with the quantum mechanical adjustment for the displaced oscillator Franck-Condon lines appears to describe fully the ACN data, alternative explanations and other issues have been raised in the past. These include (i) A Fermi resonance, topological defects or non-degeneracy in the hydrogen-bond may lead equally to a similar double peak feature in the absorption spectrum. (ii) The overall validity of the approximations involving Davydov-like adiabatic derivations may not be justifiable. (iii) Can acetanilide

be described faithfully through a one dimensional Hamiltonians? In what regards alternative explanations for the double peak, there is consensus that the experimental and theoretical work performed appears to rule most of them out. The experiments of Barthes et al. have ruled out convincingly the topological defect suggestion while also shown that the hydrogen bond non-degeneracy suggested by Austin and coworkers is not valid [29,30]. Furthermore, the analysis of Careri and Scott as well as the recent analysis of Hamm have shown that the occurrence of a Fermi resonance does not seem very likely [8,20]. The validity of the adiabatic approach used by Scott and collaborators has been also discussed, however works focused more on the general Davydov soliton problem rather that the specific acetanilide application [12,31]. Acetanilide is a narrow band solid and, as a result, the occurrence or a Davydov-like extended object is unlikely. As a result the acetanilide small polaron regime may be better analyzed either perturbatively using J as a small parameter or through the direct numerical diagonalization. Finally the issue of the true dimensionality of the ACN selftrapping phenomenon demands also attention since small polarons in one and three dimensions have quite different properties [27,32]. These issues will be addressed in the following sections.

4 Quantum analysis in the small J limit

While the semiclassical analysis is useful as well as intuitive, the mere fact that the hoping matrix element J is quite small in acetanilide allows for a complete quantum mechanical solution in the limit $J = 0$ and a subsequent use of J as a perturbation parameter [14,15]. This approach is fully quantum mechanical and thus independent of any type of approximations.

4.1 Quantum $J = 0$ limit

When the nearest neighbor coupling is zero the problem can be diagonalized exactly. The Hamiltonian becomes for $J = 0$:

$$H = \hbar\Omega \sum_{j=1}^{N}(B_j^\dagger B_j + 1/2) + \hbar\omega \sum_{j=1}^{N}(b_j^\dagger b_j + 1/2) + \chi \sum_{j=1}^{N} B_j^\dagger B_j (b_j^\dagger + b_j). \tag{24}$$

We perform the Lang–Firsov transformation [33] by introducing the unitary operator $U = e^{-S}$ where

$$S = \frac{\chi}{\hbar\omega} \sum_{j=1}^{N} B_j^\dagger B_j (b_j^\dagger - b_j). \tag{25}$$

For the diagonalization it is useful to consider the following identities:

$$U^\dagger B_l^\dagger B_l U = B_l^\dagger B_l \tag{26}$$

$$U^\dagger b_l^\dagger U = b_l^\dagger - \frac{\chi}{\hbar\omega} B_l^\dagger B_l \tag{27}$$

$$U^\dagger b_l U = b_l - \frac{\chi}{\hbar\omega} B_l^\dagger B_l \tag{28}$$

$$U^\dagger b_l^\dagger b_l U = b_l^\dagger b_l - \frac{\chi}{\hbar\omega} B_l^\dagger B_l (b_l^\dagger + b_l) + \left(\frac{\chi}{\hbar\omega}\right)^2 B_l^\dagger B_l B_l^\dagger B_l. \tag{29}$$

The transformed Hamiltonian $\tilde{H} = U^\dagger H U$ after removing the zero-point motion terms becomes

$$\tilde{H} = \sum_{j=1}^{N} \left[\left(\hbar\Omega - \frac{\chi^2}{\hbar\omega}\right) B_j^\dagger B_j - \frac{\chi^2}{\hbar\omega} B_j^\dagger B_j^\dagger B_j B_j + \hbar\omega b_j^\dagger b_j \right]. \tag{30}$$

Equation (30) may be diagonalized directly, leading in the case of one vibron to the energy spectrum:

$$E = \left(\hbar\Omega - \frac{\chi^2}{\hbar\omega}\right) + n\hbar\omega \tag{31}$$

for $n = 0, 1, 2, \ldots$. We note that the one vibron excitation has lowered its energy due to the coupling to the phonons by an amount equal to (see figure 3)

$$E_{pb} = -\frac{\chi^2}{\hbar\omega}. \tag{32}$$

The quantity E_{pb} is the polaron binding energy determined quantum mechanically in the $J = 0$ limit. This result coincides with the semiclassical polaron binding energy calculated in section (3.3).

4.2 Quantum $J \to 0$ limit

When $J \neq 0$ the unitary transformation applied to the vibron transfer term gives

$$U^\dagger H_J U = -J \sum_{j=1}^{N} (U^\dagger B_j^\dagger B_{j+1} U + U^\dagger B_j^\dagger B_{j-1} U) = -\sum_{j=1}^{N} (J_{j,j+1} B_j^\dagger B_{j+1} + J_{j,j-1} B_j^\dagger B_{j-1}) \tag{33}$$

$$J_{j,j+1} = J \exp\left\{-\frac{\chi}{\hbar\omega}\left[(b_j^\dagger - b_j) - (b_{j+1}^\dagger - b_{j+1})\right]\right\}. \tag{34}$$

In order to proceed we assume first that the system is at zero temperature and the phonons at each site are in their corresponding ground state, viz. $|0\rangle \equiv |0\rangle_{ph} = \ldots |0\rangle_{j-1}|0\rangle_j|0\rangle_{j+1} \ldots$; using this state we find an effective coupling between adjacent sites:

$$J_{\text{eff}} = \langle 0|J_{j,\,j+1}|0\rangle = J \exp\left[-\left(\frac{\chi}{\hbar\omega}\right)^2\right]. \tag{35}$$

The effective bandwidth of the polaron tunneling is thus reduced as a result of the interaction with phonons [34]. This renormalization of the polaron bandwidth is an approximate, mean field result, that ignores local phonon fluctuations and has a small effect when J is small ($J \ll \hbar\omega$). While the Lang–Firsov transformation does not depend on the value of J, the averaging over the zero phonon states should be done for small hopping matrix elements.

Using equation (35) we may now write the transformed Hamiltonian in the $J \to 0$ limit for the case of zero phonons as follows:

$$\tilde{H} = \sum_{j=1}^{N} \left[\left(\hbar\Omega - \frac{\chi^2}{\hbar\omega}\right) B_j^\dagger B_j - J_{\text{eff}}(B_j^\dagger B_{j+1} + B_j^\dagger B_{j-1}) - \frac{\chi^2}{\hbar\omega} B_j^\dagger B_j^\dagger B_j B_j\right]. \tag{36}$$

If we assume that only one $C = O$ vibron is present while phonons are in their ground state, i.e.

$$|\psi\rangle = \sum_{j=1}^{N} \psi_j B_j^\dagger |0\rangle_{ex} |0\rangle_{ph} \tag{37}$$

then we can directly diagonalized the tight-binding Hamiltonian. Using equation (37) in equation (36) leads to

$$E\psi_j = \left(\hbar\Omega - \frac{\chi^2}{\hbar\omega}\right)\psi_j - J_{\text{eff}}\left(\psi_{J+1} + \psi_{j-1}\right). \tag{38}$$

The energy spectrum for the one-vibron sector is

$$E(k) = \left(\hbar\Omega - \frac{\chi^2}{\hbar\omega}\right) - 2Je^{-\left(\frac{\chi}{\hbar\omega}\right)^2}\cos(ka). \tag{39}$$

The approximate small-J procedure leads to a small polaron band that has gained energy $-\chi^2/\hbar\omega$ with respect to the center of the bear exciton band (obtained for $\chi = 0$) and has a reduced bandwidth equal to $4Je^{-(\frac{\chi}{\hbar\omega})^2}$. This polaron band is the only one-exciton, zero-phonon solution in the $J \to 0$ limit. The approximate energy $E(k)$ for the small polaron band of equation (39) is identical to the one obtained by Scott using degenerate perturbation theory [10].

Let us briefly summarize the findings of the approximate but fully quantum mechanical treatment: In the search for the eigenstates of the Holstein Hamiltonian, the exact quantum mechanical calculation at $J = 0$ results in an eigenstate that has energy lower by an amount equal to $E_{bp} = -\chi^2/\hbar\omega$ from the bear exciton state. This state is thus favored energetically over the bear exciton that exists when $\chi = 0$. The value of the binding energy of this new polaron state coincides with the semiclassical (DNLS) binding energy. For exciton hoping J small we find (at $T = 0$) that this state acquires dispersion with bandwidth $B = 4J \exp\left[-(\chi/\hbar\omega)^2\right]$. Consequently, this solution provides the small polaron *band* formed as result of exciton-phonon coupling and the small J value. Since the semiclassical and quantum mechanical polaron binding energies are identical, we may consider that the localized semiclassical polarons begin to tunnel when quantum fluctuations are included to low order and form a band with bandwidth B. We point out that for acetanilide $B \approx 16 \exp(-1/4)\,\mathrm{cm}^{-1} \approx 12.4\,\mathrm{cm}^{-1}$, i.e. the bandwidth reduction due to exciton-phonon coupling is small.

Although the polaron solutions in the semiclassical and quantum treatments coincide, the free exciton solution found in the context of DNLS seems to be absent in the quantum mechanical analysis. It is in fact easy to see that in the fully quantum approach the exact free exciton state is not an eigensolution in any dimension since any extended exciton wave state generates phonons through the exciton-phonon coupling term in the Hamiltonian. Since the presence of the free exciton peak is central to the explanation of the acetanilide amide I spectrum one must find a way to bypass this problem. One possibility that is compatible with the semiclassical picture is to consider that the free exciton state is actually an excited polaron state that involves a number of excited phonons. However since the phonon involved in the process has energy equal to $50\,\mathrm{cm}^{-1}$ while the polaron binding energy is less than half of this value (approximately $16\,\mathrm{cm}^{-1}$), an excited polaron plus one phonon cannot match the value of $16\,\mathrm{cm}^{-1}$, except for exceptionally large values of χ that are not reasonable for molecular crystals. Another possibility is that the description of acetanilide as a one dimensional solid is not sufficient. It is known semiclassically that in $3D$ the polaron state may be separated by a barrier from the free exciton state and, as a result, both states may coexist in some fashion [27]. If such a picture survives in the fully quantum case and for the proper parameter regime, it might then be possible to identify the two states accordingly. These issues will be addressed in detail later. We note here that the small-J analysis can be done easily in three dimensions leading to a small polaron band with energy

$$E(\mathbf{k}) = \left(\hbar\Omega - \frac{\chi^2}{\hbar\omega}\right) - 2e^{-(\frac{\chi}{\hbar\omega})^2}\left[J_x \cos(k_x a_x) + J_y \cos(k_y a_y) + J_z \cos(k_z a_z)\right] \qquad (40)$$

where $\mathbf{J} \equiv (J_x, J_y, J_z)$ are the hopping rates for the three Cartesian directions respectively, $\mathbf{k} = (k_x, k_y, k_z)$ is the wavevector and $\mathbf{a} = (a_x, a_y, a_z)$ the lattice spacings.

4.3 Brief summary on various approaches

It is worthwhile to summarize briefly the various equations obtained so far through three different approaches.

- The semiclassical DNLS equation may be obtained variationally either by (a) considering phonons classical or (b) assuming that phonons are quantum but distributed according to coherent states. In both cases we obtain identical results, viz. energy gain for the polaron and no bandwidth reduction. In the Born–Oppenheimer approximation both approaches lead to identical dynamical equations as well.
- When we solve the Holstein model fully quantum mechanically but in the small hopping limit we find a polaron band with energy gain and a reduced bandwidth.

Comparing these approached we find that all three of them (pure semiclassical, phonons in coherent states as well as quantum mechanical) give the same polaron energy gain, yet, the bandwidth reduction does arise only from the fully quantum mechanical approach. Furthermore, the free exciton state is a stationary solution only semiclassically. While the semiclassical approaches result to an effective nonlinear equation of motion, viz. DNLS, the approximate quantum methodology leads to a QDNLS Hamiltonian [35]. The latter provides a fully quantum mechanical reduced description for the excitons provided the hopping rate J is small and phonons are not excited on average from their ground states.

From equation (36) we see that the on site term of the QDNLS Hamiltonian contains already the polaron binding energy shift while the hopping term is also renormalized. When only one exciton is present, this Hamiltonian describes a small polaron band. When more exciton quanta are present, it may describe multiexciton states as well as interaction among them. It is clear that the QDNLS approach is valid when intersite phonon correlations are not important.

5 The free exciton state in the semiclassical analysis

In order to focus deeper into the double peak acetanilide structure we may investigate in more detail the semiclassical picture before ultimately probe directly the fully quantum regime using exact numerics. In this section we will look into the free exciton state both in the Born-Oppenheimer approximation in one dimension but also treating the three dimensional case.

5.1 Born–Oppenheimer approximation

In the fully adiabatic picture the classical Einstein oscillators of the Holstein Hamiltonian have no dynamics but follow the exciton motion. We may still consider these oscillators classical but allow them a characteristic time scale for response to the exciton motion. In this case we need to solve the set of equations (13),(14) that determine the stability of the adiabatic solutions. The acetanilide values correspond to $\alpha \approx 2.3$ and $\gamma \approx 10$; thus if we substitute the semiclassical adiabatic solutions for the small polaron and free exciton of section 2.3 and use equations (13),(14) we will find what is the regime of stability of these solutions. The adiabatic polaron state may be constructed via a numerically exact procedure from the anticontinuous limit; its linear stability has already been discussed [27]. The stability of the free exciton state, on the other hand, may be assessed numerically by direct substitution of the state in the equations of motion of equations (13), (14); the result is shown in figure (4). In order to engage the vibrational lattice to the free exciton we have added initially a small component of uniform noise in the classical phonons. In the figureure we show the free exciton evolution in time units $t_{ex} = \gamma\tau/5 \equiv Jt/5$; we observe that after few exciton oscillations the free exciton becomes unstable and forms localized structures. The phenomenon of the semiclassical polaron formation from the free exciton state is controlled by a characteristic polaron formation time τ_p. This waiting time for the onset of localization depends strongly on the specific parameter regime as well as initial amplitude to the phonon excitation. Extensive simulations show that $\tau_p \to \infty$ when $\gamma \to 0$, i.e. when we address the fully adiabatic regime. In the opposite limit of $\gamma > 1$, on the other hand, the semiclassical free exciton becomes very quickly unstable and localizes. We expect that as the temperature of the system increases, this effect becomes more dominant leading to a collapse of the free exciton into localized states.

The use of a finite parameter $\gamma = \hbar\omega/J$ in the semiclassical problem introduces a new time scale in the Holstein Hamiltonian; while τ is the natural time scale for the phonon evolution (measured in phonon periods) , the exciton time is measured in $\tau_{ex} = \gamma\tau$. In the adiabatic regime $\gamma \ll 1$ and in the course of many exciton oscillations there are very few phonon circles. Using in equations (13),(14) as initial condition a free exciton state, we observe that the slow phonon change simply modifies the local site energies of the exciton equation; as a result the free exciton suffers very weak phonon perturbation and survives for long times. In the opposite regime where $\gamma \gg 1$, many phonon oscillations occur in few exciton ones; as a result the interaction term acts as an effective multiplicative noise term (for some initial phonon conditions) leading to a very
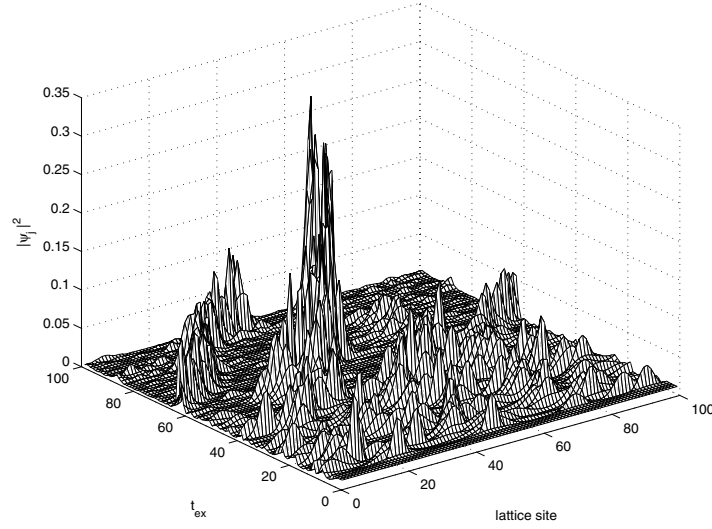
Fig. 4. Time evolution of the site probability $|\psi_j|$ as a function of exciton time $t_{ex} = \tau/5\gamma \equiv Jt/5$ for $\gamma = 10$ and $\alpha = 2.3$. We used a periodic one dimensional lattice of 100 sites. The initial condition is that of a free exciton of zero momentum and uniform noise in the initial (dimensionless) phonon displacements u_j's with amplitude of the order of 10^{-3} (the phonon lattice evolution is not shown). The free exciton is initially stable but subsequently collapses to localized states.

rapid collapse of the free exciton into localized states. This purely classical effect is enhanced in the fully quantum regime through the zero point motion.

Since the parameter regime of acetanilide is in the range $\gamma > 1$ we find that the free exciton is generally unstable to even quite small perturbations. This behavior poses a problem to the standard one dimensional adiabatic explanation since, for this approach to be valid the free exciton state should be stable as is the small polaron. One way to proceed within the semiclassical context is to consider the possibility that the selftrapping phenomenon takes place in three dimensions. Since, as noted earlier, in 3D a barrier separates free exciton and polaron, it may be that the barrier helps in stabilizing both states [27]. We will proceed with the semiclassical analysis of the 3D Holstein model in the next subsection.

5.2 Semiclassical 3D problem

It was pointed out recently that the dipole-dipole interaction responsible for the nearest-neighbor transfer of excitons in ACN extends not only along the hydrogen-bonded chain direction but also in the plane perpendicular to it [36]; this point will be detailed in sections 6 and 7.1. In order to perform the semiclassical analysis for the general problem in three dimensions we write the semiclassical Holstein Hamiltonian as follows:

$$H_{sc} = \sum_{\mathbf{j}} \left[\hbar\Omega|\psi_{\mathbf{j}}|^2 - (\Delta\psi)_{\mathbf{j}} + \hbar\omega b_{\mathbf{j}}^* b_{\mathbf{j}} + \chi|\psi_{\mathbf{j}}|^2(b_{\mathbf{j}}^* + b_{\mathbf{j}}) \right] \tag{41}$$

$$(\Delta\psi)_{\mathbf{j}} = J_x \left(\psi_{j_x,j_y,j_z}^* \psi_{j_x+1,j_y,j_z} + \psi_{j_x,j_y,j_z}^* \psi_{j_x-1,j_y,j_z} \right)$$

$$J_y \left(\psi_{j_x,j_y,j_z}^* \psi_{j_x,j_y+1,j_z} + \psi_{j_x,j_y,j_z}^* \psi_{j_x,j_y-1,j_z} \right)$$

$$+ J_z \left(\psi_{j_x,j_y,j_z}^* \psi_{j_x,j_y,j_z+1} + \psi_{j_x,j_y,j_z}^* \psi_{j_x,j_y,j_z-1} \right) \tag{42}$$

where $\mathbf{j} = (j_x, j_y, j_z)$ and J_x, J_y, J_z are the transfer rates in the three perpendicular axis directions. We assume that the hydrogen bonded axis coincides with the x-axis; the parameters J_x, J_y, J_z may take positive (negative) values leading to negative (positive) hopping

rates. We may now perform the variational minimization with respect to the phonon c-numbers $b_{\mathbf{j}}^*$, $b_{\mathbf{j}}$ and obtain the variational energy E_v:

$$E_v = \sum_{\mathbf{j}} \left[\hbar\Omega|\psi_{\mathbf{j}}|^2 - \frac{\chi^2}{\hbar\omega}|\psi_{\mathbf{j}}|^4 - J_x \left(|\psi_{j_x+1,j_y,j_z} - \psi_{\mathbf{j}}|^2 - 2 \right) \right.$$
$$\left. - J_y \left(|\psi_{j_x,j_y+1,j_z} - \psi_{\mathbf{j}}|^2 - 2 \right) - J_z \left(|\psi_{j_x,j_y,j_z+1} - \psi_{\mathbf{j}}|^2 - 2 \right) \right] \qquad (43)$$

where d is the dimensionality. In order to probe into the variational energy E_v we make the ansatz

$$\psi_{\mathbf{j}} = A\zeta^{|j_x|}\eta^{|j_y|}\theta^{|j_z|} \qquad (44)$$

where $|\zeta| \leq 1$, $|\eta| \leq 1$, $|\theta| \leq 1$. The three parameters ζ, η, and θ take positive (negative) values when the hopping overlap in the corresponding direction is negative (positive). The normalization factor is found to be

$$A = \left(\frac{1-\zeta^2}{1+\zeta^2} \right)^{1/2} \left(\frac{1-\eta^2}{1+\eta^2} \right)^{1/2} \left(\frac{1-\theta^2}{1+\theta^2} \right)^{1/2}. \qquad (45)$$

Substitution of the trial function of equation (44) into equation (43) we obtain the following expression for the variational energy

$$E_v = -4 \left[J_x \frac{\zeta}{1+\zeta^2} + J_y \frac{\eta}{1+\eta^2} + J_z \frac{\theta}{1+\theta^2} \right]$$
$$- \frac{\chi^2}{\hbar\omega} \frac{(1-\zeta^2)(1+\zeta^4)}{(1+\zeta^2)^3} \frac{(1-\eta^2)(1+\eta^4)}{(1+\eta^2)^3} \frac{(1-\theta^2)(1+\theta^4)}{(1+\theta^2)^3}. \qquad (46)$$

In the fully symmetric case of $J_x = J_y = J_z \equiv J > 0$ we have $\zeta = \eta = \theta \equiv \eta$ and obtain the general expression d dimensions [27]

$$E_v = -4dJ\frac{\eta}{1+\eta^2} - \frac{\chi^2}{\hbar\omega} \frac{(1-\eta^2)^d(1+\eta^4)^d}{(1+\eta^2)^3d}. \qquad (47)$$

Figure 5 shows the variational energy (in units of J) in 1D and 3D for the isotropic case with all negative hopping overlaps ($J > 0$). In 1D, the curve is barrierless for any set of parameters, regardless how small the coupling is. That is, a partially localized solution $\eta < 1$ has always smaller energy than the extended solution $\eta = 1$, and furthermore, this solution can be reached without having to surmount any barrier. The behavior in 3D is drastically different. For couplings below the critical threshold value $\alpha_c \equiv \sqrt{2\chi_c^2/\hbar\omega J} = 3.288$, the extended solution with $\eta = 1$ is the lowest energy solution. For couplings larger than this critical value α_c, a strongly localized state $\eta \ll 1$ becomes the lowest energy solution [27].

5.3 Polaron and free exciton coexistence in three dimensions

The effective semiclassical barrier between the free exciton and small polaron forms when $\alpha = \alpha_c \approx 3.288$. When $\alpha < \alpha_c$ the minimum energy state is the free exciton while for $\alpha > \alpha_c$ is the small polaron. When the parameter values are such that an adiabatic double well structure is formed, the transition from free exciton to small polaron occurs through quantum lattice fluctuations. A simple way to include the latter while retaining the intuitive adiabatic picture is by treating η as an effective "configureurational variable" and quantizing the double well potential problem. In other words, we may consider that the dynamics of the transition between polaron and exciton may be described by a particle of effective mass m^* that is moving in the adiabatic potential. Upon diagonalization of this effective one dimensional problem we may obtain the states involved and understand their dynamics. The results are shown in figure 6 for $\alpha = 4$ where we portray the adiabatic potential, the four lowest energy eigenvalues as well

as the three lowest eigenfunctions. The equilibrium position is zero for the undisplaced free exciton state. For the parameter regime shown the lowest potential minimum corresponds to the small polaron while the smooth, wide secondary minimum is the free exciton minimum.

Fom the numerical solution of the spectral problem we find that the two lowest states are relatively close in energy and form a type of doublet. The ground state wavefunction has a single peak that appears to have two components. While it is centered close to the polaron minimum it has a considerable overlap with the exciton minimum as well. The first excited state, on the other hand, is doubly-humped and centered in the wide, shallow secondary minimum of the free exciton but with significant amplitude in the polaron minimum. The ground state-excited state doublet has distinct polaron-like and exciton-like structure respectively. If the $3D$ Holstein model is a good representation of the acetanilide problem, then it is possible that these are the two states that are relevant for the explanation of the double peak in the ACN absorption spectrum.

In the previous analysis we used a relatively large value of the nonlinearity parameter so that we are withing the double well regime of the adiabatic potential. This choice may be justified in the following way: Since we know that in reality the polaron hopping rate is reduced we may in an ad-hoc fashion use the effective rate of equations (35) instead of just J and obtain a new nonlinearity parameter $\alpha_{\mathrm{eff}} = \exp\left[\frac{1}{2}(\frac{\chi}{\hbar\omega})^2\right]\alpha$ that is larger than α. This way the effective nonlinearity increases for the same acetanilide values and the system is found to be closer to the adiabatic double well regime. Clearly further investigation on this approach is necessary.

6 Numerically exact diagonalization of the Holstein Hamiltonian

With recent advances in computer technology it became possible to diagonalize the Holstein Hamiltonian on a numerically exact level, even in the 3D case [37,38]. This allows one to study to what extent the conclusions from the DNLS (e.g. the existence of a barrier in the 3D case) manifest itself in the full quantum regime. To that end, a concept introduced by Trugman and coworkers is used [37,38]. In brief, Bloch states with momentum k are constructed:

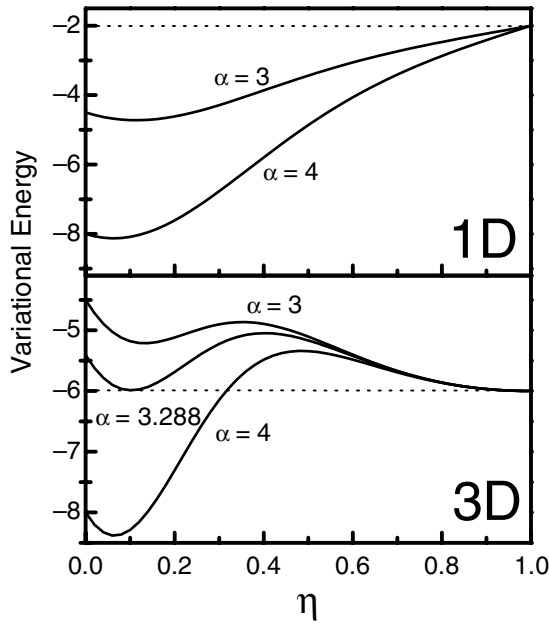$$\psi = \frac{1}{\sqrt{N}} \sum_j \Phi e^{ikj} \qquad (48)$$

Fig. 5. Variational energy in 1D (top) and 3D (bottom) for various values of the parameter $\alpha \equiv \sqrt{2\chi^2/\hbar\omega J}$. Adapted from [27].
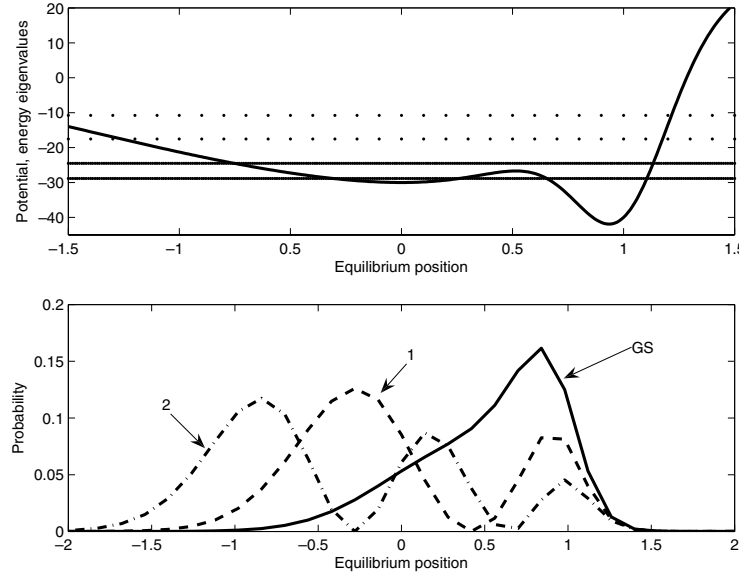
Fig. 6. (a) The adiabatic potential for the 3D polaron as a function of displacement; the horizontal lines correspond to the first two energy eigenvalues while dots the next two for $\alpha = 4$ and $m^* = 5$. In (b) the spatial distribution of the probability for the lowest three eigenfunctions, the ground state (GS), first (1) and second (2) excited states, respectively.

with site states Φ that are identical for each site j. The site states are expanded in a basis $\varphi_{\{n_i\}}$:

$$\Phi = \sum_{\{n_i\}} c_{\{n_i\}} \varphi_{\{n_i\}} \tag{49}$$

with (in one dimension):

$$\varphi_{\{n_i\}} = |1_0; \ldots, n_{-1}, n_0, n_{+1}, \ldots\rangle \tag{50}$$

where the '1_0' denotes that we have one quantum in the exciton coordinate at site 0 (since the Hamilton is quantum-conserving with respect to the exciton coordinate, it is block-diagonal and we consider here only the one-quantum manifold of states). The n_i are the numbers of phonon excitations at site i around the exciton at site 0.

The essential trick of [37,38] is an efficient strategy to select basis states, which we review here only very briefly. We start from a 'root' basis state without any phonon excitation: $|1_0; \ldots, 0, 0, 0, \ldots\rangle$. For each generation (total number of generations: N_h), basis states are added corresponding to jumps along one of the off-diagonal elements of the Hamiltonian equations (2)–(4) in a tree-like manner. This can either be one phonon jump with a matrix element

$$\langle 1_0; \ldots, n_{-1}, n_0, n_{+1}, \ldots |H| 1_0; \ldots, n_{-1}, n_0 + 1, n_{+1}, \ldots\rangle = -\sqrt{n_0 + 1}\chi \tag{51}$$

or a shift along one of the crystal directions with matrix elements

$$\langle 1_0; \ldots, n_{-1}, n_0, n_{+1}, \ldots |H| 1_0; \ldots, n_{-2}, n_{-1}, n_0, \ldots\rangle = J \exp(ika). \tag{52}$$

In optical spectroscopy, where a $k = 0$ selection rule exists, the phase factor $\exp(ika)$ disappears. The basis gets a pyramidal shape with maximum N_h phonon excitations at site 0 to one phonon excitation at one site $\pm(N_h - 1)$ in either lattice direction. The basis is infinite with respect to lattice transformations and fully accounts for the translational symmetry of the crystal
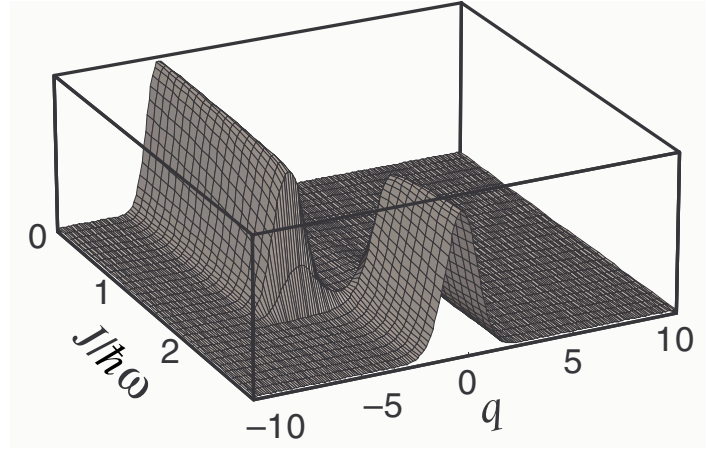
Fig. 7. The Holstein Hamiltonian in 3D with isotropic negative exciton coupling: Projection of the ground state wavefunction onto the phonon-coordinate q. The exciton-phonon coupling was set to $\chi/\hbar\omega = 3.5$ in this calculation, and the exciton coupling $J/\hbar\omega$ was varied from 0 to 3.

(equation (48)). However, the basis is finite with respect to the phonon-exciton distance, and the phonons are confined to the exciton by construct within $\pm(N_h - 1)$. The number of basis states scales as $O\left((D+1)^{N_h}\right)$, where D is the dimensionality of the system. In 3 dimensions with generation number $N_h = 11$, this reveals as many as 1.4×10^6 basis states. Nevertheless, the matrix is sparse and can be partially diagonalized using a Lanczos algorithm. On an AMD Opteron processor with 12 GB main memory, the ground state is calculated within minutes, or, if the whole absorption spectrum is needed, within typically a day.

Before we start, one comment is in order: In order to distinguish a free-exciton from a polaron solution, we will use the phonon displacement q as a criterion. It might seem more logical to investigate the extension of a solution in real space, similar to in the DNLS case (section 5.2). However, even though the free-exciton would, of course, be perfectly delocalized in real space, any polaron solution would be as well in the full-quantum case and one could not distinguish between polaron and exciton in this way. This is by construct of the Bloch ansatz equation (48), which accounts for the translational symmetry of the problem. In the strict meaning of the word, there is no true, spatial self-trapping in the full-quantum case. This is fundamentally different from the semi-classical DNLS case, which does break the translational symmetry of the problem and reveals solutions that are localized in real space. Only in the limit of infinite effective polaron mass, where the polaron-dispersion relation would becomes infinitely flat, one could construct spatially localized wavepackets, which then would indeed be eigenstates of the polaron Hamiltonian. Comparison with equation (39) shows that a flat dispersion relation is obtained for $\chi/\hbar\omega \to \infty$.

Figure 7 shows the results of a numerically exact matrix diagonalization of the Holstein Hamiltonian for exciton-phonon coupling $\chi/\hbar\omega = 3.5$ with the exciton coupling $J/\hbar\omega$ varied from 0 to 3. Shown is the projection of the corresponding ground state wavefunction onto the phonon coordinate q. With this set of parameters, the system should be close to the DNLS regime ($\chi/\hbar\omega \gg 1$), so one expects that one can directly compare results from section 5.2 with that from the exact diagonalization.

Indeed, for small exciton phonon couplings J, which corresponds to a large $\alpha \equiv \sqrt{2\chi_c^2/\hbar\omega J}$, the wavefunction is displaced with respect to the phonon coordinate, close to the value $\sqrt{2}\chi/\hbar\omega$ expected from the displaced oscillator picture (section 4.1). Referring to figure 5, this corresponds to a polaron solution with small η for $\alpha > \alpha_c$, which in this parameter range constitutes the lowest energy solution. However, as the exciton coupling is increased to $J/\hbar\omega \approx 2.2$, which for the given exciton-phonon coupling relates to the critical value $\alpha_c = 3.288$, the ground state wave function jumps almost suddenly back to $q \approx 0$. From figure 5 we expect for $\alpha < \alpha_c$ that the extended state with $\eta = 1$ becomes the lowest energy solution, and accordingly, the
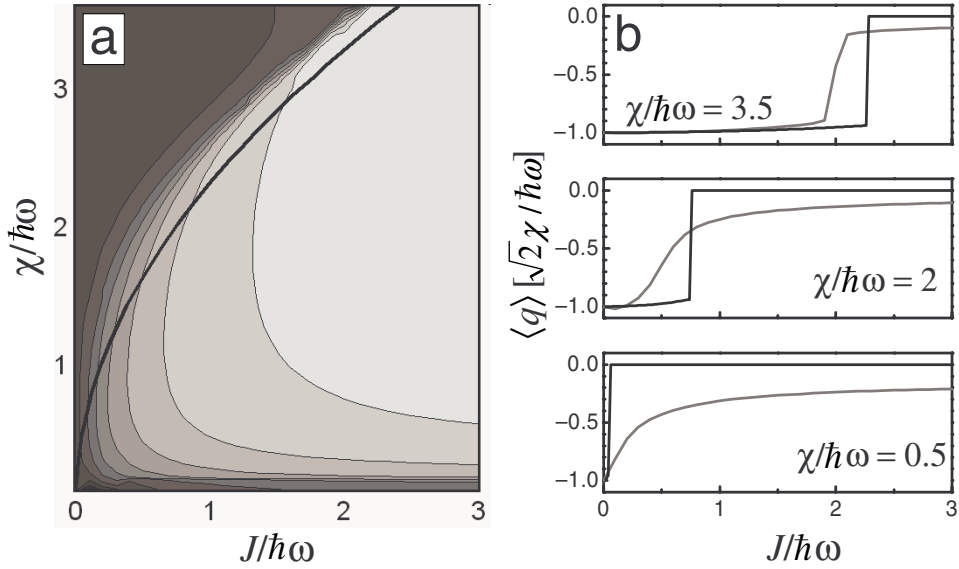
Fig. 8. The Holstein Hamiltonian in 3D with isotropic negative exciton coupling: (a) Displacement of the phonon coordinate q (in units of $\chi/\hbar\omega$) of the ground state according to a full-quantum diagonalization of the Holstein Hamiltonian. Results are plotted as a function of exciton coupling J and exciton-phonon coupling χ, both in units of the phonon frequency $\hbar\omega$. The thick line separates the two regimes predicted from the semi-classical DNLS: $\alpha_c = \sqrt{2\chi_c^2/\hbar\omega J} = 3.288$ (b) Horizontal cuts through (a), exemplifying the quantum case (bottom, $\chi/\hbar\omega = 0.5$), the close to classical case (top, $\chi/\hbar\omega = 3.5$), and an turn-over regime (middle, $\chi/\hbar\omega = 2.0$). The grey lines represent the results from an exact diagonalization, the black lines that from the DNLS, interpreting the interaction term in equation (11) as an effective coupling $\chi_{\text{eff}} = \chi|\psi|^2$; hence the maximum displacement found in the peak of the wavefunction is $q = \sqrt{2}\chi|\psi_{max}|^2/\omega$. In either case, the displacement q is plotted in units of $\sqrt{2}\chi/\hbar\omega$.

phonon-displacement q vanishes at this point. If the system were truly classical, the switching between the two regimes would occur instantaneously, but since the quantum mechanical wavefunction delocalizes, a relatively small parameter regime exists where polaron and exciton solutions coexist (similar to figure 6). However, we note that even though exciton-like solutions are found in the quantum case, they are not exactly free excitons (the displacement q is not exactly zero). The free exciton is not an eigenstate of the Holstein Hamiltonian.

Figure 8(a) puts these results into a more general perspective. Shown is the expectation value of the phonon displacement $\langle q \rangle$, relative to that expected from the $J = 0$ case $q_{max} = \sqrt{2}\chi/\hbar\omega$, as a function of the two parameters of the theory $\chi/\hbar\omega$ and $J/\hbar\omega$. The thick line separates the two regimes of the semi-classical DNLS, defined by $\alpha_c \equiv \sqrt{2\chi_c^2/\hbar\omega J} = 3.288$: Left from that line, the DNLS predicts polaron solutions with displacements close to the maximal value $q_{max} = \sqrt{2}\chi/\hbar\omega$, whereas extended states with $\eta = 0$ are expected on the right side of this phase diagram. For larger exciton-phonon coupling, $\chi/\hbar\omega > \approx 2$ the quantum solution essentially follows that line, except that the turn over between polaron and exciton solution is not discontinuous (as discussed above). Nevertheless, as $\chi/\hbar\omega$ is increased from 2 to 3.5 (figure 8(b) middle and top), the transition occurs more and more abruptly.

In contrast, for $\chi/\hbar\omega < \approx 1$ the quantum solution deviates strongly from the DNLS prediction. In particular, polaron solutions with large displacements $\langle q \rangle$ may exist even for relatively large exciton coupling J, where the DNLS would strictly reveal an exciton solution (figure 8(b), bottom). This difference between semi-classical and quantum result can be rationalized by taking into account the second term of equation (39),

$$-2J \exp\left[-\chi^2/(\hbar\omega)^2\right] \cos(ka) \tag{53}$$

which may be considered a quantum-correction factor relative to the polaron binding energy in the semiclassical DNLS case (equation (31)). The origin of the quantum-correction factor is exciton tunneling that occurs when a spatially localized solution (section 4.2) starts to delocalize due to a non-zero exciton coupling $J \neq 0$. In that case, a phonon displacement follows the exciton as the latter hops from one site to the next. In fact, the factor $\exp(-\chi^2/(\hbar\omega)^2)$ equals the overlap integral (Franck-Condon factor) for this hopping with the phonon coordinate in its quantum mechanical ground state (see equation (35)). For large exciton-phonon coupling, we have $\exp(-\chi^2/(\hbar\omega)^2) \to 0$, and equation (39) would equate equation (31). In that limit, the polaron dispersion relation would become flat (i.e. the polaron energy would be independent on wavevector k), and truly spatially localized solutions, as we obtain them from the DNLS, could indeed be eigensolutions of the quantum Hamiltonian. This is the classical limit, where tunneling is not possible and the hopping probability becomes zero! However, for small exciton-phonon coupling, the polaron energy is lowered by an additional term $2J\exp(-\chi^2/(\hbar\omega)^2)$, which may render the polaron more stable than the exciton, even when the DNLS would predict the opposite.

It is instructive to compare the results of this chapter with those of the coherent state treatment. We have seen in section 3.2 that the product ansatz equation (15) and (16) directly leads to the semiclassical DNLS without invoking any further approximation. The DNLS, however, fails in certain parameter regimes where $\chi/\hbar\omega <\approx 1$. The essential difference between coherent state treatment and the approach discussed above is that the latter uses a much larger basis (equations (48) and (50)). In particular, the 'basis' of the coherent state treatment is local in the sense that the polaron is confined to the exciton by construct. In contrast, the basis equations (48) and (50) allows phonon excitations away from the exciton with, e.g. a phonon sitting at site 1, while the exciton is sitting at site 0 at the same moment (i.e. $n_{+1} = 1$). Counterintuitively, that phonon at site 1 does *not* interact with the part of the exciton that is also residing on site 1 when shifting Φ (equation (49)) by one site along the lines of the Bloch ansatz equation (48). There is no classical counterpart to this phenomenon; it reflects the non-local character of quantum mechanics. In the limit $\chi/\hbar\omega \gg 1$, the nonlocal character become less important, and the DNLS becomes a good approximation.

7 Pump-probe experiments on ACN

7.1 Experimental results

With these introductory words in mind, we now turn to our recent femtosecond pump-probe experiments on the C=O band of crystalline ACN [20, 21]. (The pump-probe response of the NH band of ACN has been studies as well [19, 22], which however shall not be discussed here.) In such a pump-probe experiment, the various modes are first excited with an intense short IR laser pump pulse, and the response upon that excitation is then probed by a second short, but much weaker probe-pulse. The information gain of femtosecond pump-probe experiments, as compared to simple IR absorption spectroscopy (figure 2), is manifold:

- The anharmonicities of the individual modes can be measured, as sketched in figure 9(b): When pumping a state, its first excited state is populated, and the probe pulse is then probing both the 1–2 upward transition and the 1–0 downward transition. If the state is harmonic, both upward and downward transition appear at exactly the same frequency, but with opposite signs, and cancel each other exactly. In contrast, if the state is anharmonic, they lead to two bands with alternating signs separated by the anharmonicity of the transition.
- If two states are coupled, excitation of the one state will lead to an response (frequency shift) of the other. It shows to what extend the various transitions are entangled, or whether they can be viewed as separated problems. If, for example, the two lines in ACN would originate from molecules in different conformations or surroundings (topological defects), as has been suggested various times [29, 39], pumping of the one state would not cause any response of the other state (in contrast to what is seen in the experiment). On the other hand, in the
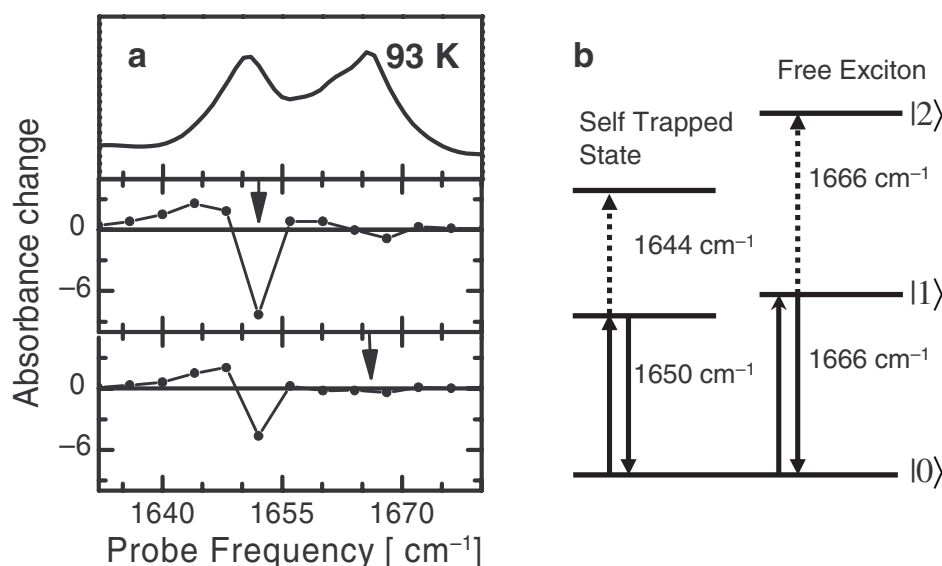
Fig. 9. (a) Linear absorption spectrum (top) and pump probe spectra of the C = O mode of crystalline ACN at 93 K for two different narrow band pump pulses chosen to be resonant with each of the absorption bands. The arrows mark the center frequency of the pump pulse, which was spectrally narrow enough to pump only either one of the transitions. (b) Level scheme of the system, explaining the distinctively different response of both modes. Adapted from [20].

case of a Fermi-resonance, another often discussed alternative explanation of the doublet in the ACN spectrum [40], a very characteristic coupling pattern is expected. Investigating such coupling patterns in detail, compelling evidence against both of these possibilities could be provided [21].
– The lifetime of the pumped states can be measured with femtosecond time resolution. In this way, the original idea of Davydov [4] can be tested, namely to what extent vibrational self-trapping may stabilize the excitation for timescales that would allow to make the energy available for subsequent biological processes.

Figure 9(a) shows the result of pump-probe experiments on the two bands of crystalline ACN [20]: When resonantly pumping the "anomalous" band (1650 cm^{-1}) of ACN, the band bleaches (negative response) and a positive band emerges at 1644 cm^{-1}. In contrast, when resonantly pumping the "normal" band (1666 cm^{-1}), hardly any bleach of the band itself is observed. Nevertheless, the anomalous band does responds with a signal which is similar in shape, but is slightly smaller than when pumping it directly.

In a somewhat heuristic approach, Edler et al. have discussed the distinctly different responses of the two bands of ACN in [20]. The self-localized state was treated along the lines of Scott's theory [41], which would relate the anharmonicity of the anomalous band to the $-\chi^2/\hbar\omega B_j^\dagger B_j^\dagger B_j B_j$ term in equation (36). At the same time, it was assumed that one can 'cut out' the exciton part of the Hamiltonian H_{ex} (equation 2) from the remainder by writing:

$$H_{ex} = \hbar\Omega \sum_{j=1}^{N} (B_J^\dagger B_j + 1/2) - J \sum_{j=1}^{N} (B_j^\dagger B_{j+1} + B_j^\dagger B_{j-1}).$$ (54)

The discussion of the exciton is a little more involved: It turns out that, apart from the artificial separation from the phonon/polaron part, this Hamiltonian is not a very realistic description of molecules. A chemical bond is not harmonic in reality, but is better described by a Morse-potential. Vibrations of real-worlds molecules are intrinsically anharmonic (on-site anharmonicity). For example, the anharmonicity of a C=O vibrator, defined as the difference in frequency of the 0–1 and the 1–2 transition, lies between 10–20 cm^{-1}. Hence, we should use instead for
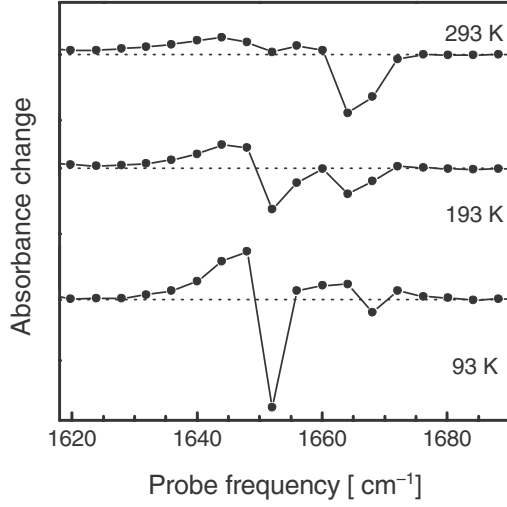
Fig. 10. Pump-probe spectra of the C=O mode of crystalline ACN as a function of temperature from 93 K to room temperature. Adapted from Ref. [20].

the exciton Hamiltonian:

$$H_{ex} = \hbar\Omega \sum_{j=1}^{N}(B_J{}^{\dagger}B_j + 1/2) - \Delta \cdot B_j{}^{\dagger}B_j{}^{\dagger}B_j B_j - J\sum_{j=1}^{N}(B_j{}^{\dagger}B_{j+1} + B_j{}^{\dagger}B_{j-1}) \qquad (55)$$

where Δ is the on-site anharmonicity. Note that the additional term does not affect the one-exciton states nor any polaron solution in the one-exciton manifold where $B_j{}^{\dagger}B_j{}^{\dagger}B_j B_j = 0$, which is why we normally can ignore it. It also doesn't affect the outcome of normal absorption spectroscopy along the lines of figure 2. The term however does affect the way how one potentially sees one-exciton states in pump-probe spectroscopy, since the two-exciton manifold is reached in such experiments.

In light of this discussion, the experimental result shown in figure 9(a), bottom, is in fact surprising. In this experiment, a vibrational state (the higher frequency band) is pumped, but cannot be depleted. Similar pump-probe experiments have been done by Hamm and coworkers on hundreds of molecules, but a result of this sort has never been obtained. 'Normal' vibrational states are intrinsically anharmonic, and as a result, one expect to see a pump-probe response similar to that of the 'anomalous' band, i.e. a bleach/stimulated emission at its original 0–1 position and a positive 1–2 absorption frequency shifted by the intrinsic anharmonicity Δ. In [20,21], several alternative explanations have been excluded, and the only possible explanation left over was: The higher frequency peak in the absorption spectrum of ACN behaves as if it were harmonic, despite the fact that it is composed of C=O vibrators that are intrinsically anharmonic. Only if the state is effectively harmonic, upward and downward transitions in figure 9(b) could cancel exactly and the zero-response seen in the experiment is expected.

Interestingly, one indeed finds that an exciton may behave effectively harmonic even in the presence of on-site anharmonicity, provided its delocalization length is sufficiently long. In fact, one can show by a perturbative expansion of the Hamiltonian equation (55), treating the anharmonicity Δ as small, that the effective anharmonicity of an exciton scales like the so-called participation ratio [20]:

$$\Delta_{\text{eff}} = \Delta \sum_{j} \Psi_j^4 \qquad (56)$$

where Ψ_j are the expansion coefficients of the exciton in a site basis. The participation ratio is a commonly used measure of the degree of delocalization, i.e. $\sum_j \Psi_j^4 = 1$ for a fully localized state and $\sum_j \Psi_j^4 \to 0$ for a perfectly delocalized state. The exciton's anharmonicity is a direct measure of its degree of delocalization which, according to figure 9(a), bottom, is large at 93 K.

Interesting in this context is the temperature dependence of this effect (figure 10): At low temperatures, in the absence of disorder, the exciton is fully delocalized, and one can

hardly bleach it. However, as temperature rises, disorder increases and the exciton starts to Anderson-localize. As a result, the exciton transition could then indeed be bleached because its effective anharmonicity increases (figure 10, top). The onset of disorder-induced Anderson localization of the free exciton is observed at about the same temperature where the intensity of the self-trapped state disappears. This finding suggests that both localization mechanisms are connected. Disorder localization is caused by random variations of the diagonal elements of the excitonic coupling Hamiltonian equation (55). The amide I frequency is known to vary significantly with hydrogen bond distance (on the order of 20–$30 \, \mathrm{cm}^{-1} \, \mathrm{\AA}^{-1}$); hence, thermal excitation of phonons that give rise to random fluctuations of the hydrogen bond distances lead to disorder-induced localization of the free exciton. Since these are exactly the phonons which also mediate self-trapping at low temperatures, thermal excitation at the same time diminish the intensity of the self-localized state. Hence, it is the same nonlinear interaction, the variation of the amide I excitation energy with hydrogen bond distance, which gives rise to the two effects: (i) diagonal disorder and as a consequence, disorder-induced localization of the free exciton with rising temperature and (ii) self-localization at sufficiently low temperatures. The competition between Anderson (disorder) localization and nonlinear self-localization in the presence of disorder has been investigated in [42]: Those states that are self-localized for large enough nonlinear exciton-phonon coupling χ are quite distinct from those that are Anderson (disorder) localized. Upon reducing the nonlinear coupling, the self-trapped states become less localized and eventually reach bifurcation points, below which they do not exist. Surprisingly, the states that are Anderson localized for vanishing nonlinear coupling become rapidly delocalized and unstable as nonlinear coupling is increased just slightly.

Hamm and coworkers [20] concluded that the pump-probe experiments are fully consistent with earlier interpretations of conventional temperature dependent absorption spectroscopy [10], namely that the higher frequency band of ACN relates to an free exciton whereas the lower frequency band relates to a self-localized state. Nevertheless, it turns out that the lifetime of either of these sates is short, $2 \, \mathrm{ps}$ [20], and as such, the original idea of Davydov [4] that vibrational self-trapping stabilizes the excitation, did probably *not* come true. A lifetime of 2 ps is a typical value for vibrational energy dissipation in condensed phase systems, and vibrational self-trapping is not capable to extend this lifetime by any significant amount. 2 ps appears to be too short to trigger any serious conformational transition of a protein that could potentially be important in the biological function of the system.

7.2 Comparison to a numerically exact theory

Although the discussion outlined above seemed to explain the experiment conclusively, we note again that the 'theory' of [20] artificially tried to 'cut out' the exciton part from the remainder. At the same time, it is clear that the free exciton is not an eigenstate of the full Hamiltonian equation (1)–(4), which can be seen from simple insertion. Furthermore, also the experiments show that exciton and polaron are, of course, coupled to each other, leading to a spectral response of the latter when pumping the former (figure 9(a), bottom). Unfortunately, none of the limiting regimes discussed in the previous sections apply to the parameter range that has been proposed for the ACN problem ($\chi \approx 25 \, \mathrm{cm}^{-1}$, $\omega \approx 50 \, \mathrm{cm}^{-1}$, $J = 4 - 10 \, \mathrm{cm}^{-1}$):

- The DNLS (section 3 and 5.2) is valid in the limit $\chi/\hbar\omega \to \infty$, in which case the polaron binding energy $E_b = -\chi^2/\hbar\omega$ would become large compared to the discreteness of the oscillation frequency $\hbar\omega$. However, for the given set of parameters for ACN we find $\chi/\hbar\omega = 0.5$; by no means large! In fact, figure 8 shows that polaron solutions are expected in this regime for relatively large exciton couplings J, where the DNLS would strictly predict exciton solutions.
- The small J limit seems to be better justified (section 4.1 and 4.2). Yet, this limit does not predict the existence of a free exciton, in disagreement with the common picture of the spectroscopy of ACN, and in disagreement with the interpretation of the experimental pump-probe results discussed above. According to the small J limit, one would rather expect a first excited state that lies exactly one phonon quantum above the ground state (equation (31)).
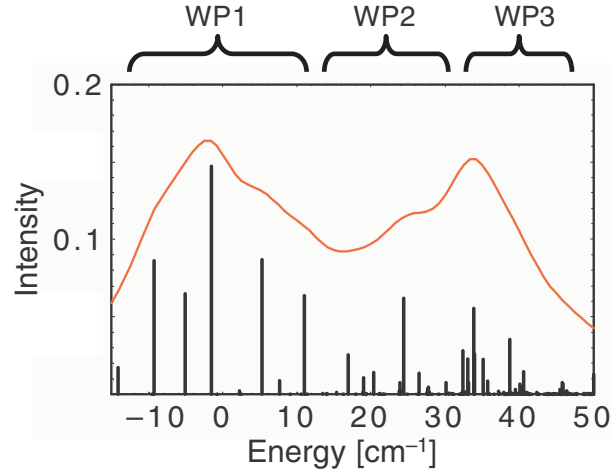
Fig. 11. Absorption spectrum of the Holstein in 3D with $\hbar\omega = 50\,\text{cm}^{-1}$, $\chi = -25\,\text{cm}^{-1}$, $J_\parallel = 10\,\text{cm}^{-1}$ and $J_\perp = -10\,\text{cm}^{-1}$. Stick spectra and spectra convoluted with a Lorentzian lineshape function with width $10\,\text{cm}^{-1}$ (FWHM) are shown. The eigenstates appear in clusters with properties of a polaron in its ground state (WP1), an exciton in its ground states (WP2), and a polaron in its first excited state (WP3, see figure 12). Adapted from [36].

However, a hypothetical phonon frequency of $\omega = 15\,\text{cm}^{-1}$ (the spacing between two bands in figure 2) would result in a completely different temperature dependence with a much lower turn-over between low and high temperature regime [10], and would furthermore contradict the experimental observation that it is indeed a $\omega = 50\,\text{cm}^{-1}$ phonon that couples strongly to the hydrogen bond [19,22].

The existence of the two solutions of the DNLS, an extended free exciton and an self-localized small polaron, was commonly used to rationalize the two peaks in the absorption spectrum of ACN (figure 2(a)). According to this interpretation, the lower frequency band relates to a self-trapped state with a temperature dependence given by the displaces oscillator picture [13,14,10] while the higher frequency band relates to the free exciton. Again, the free exciton is *not* an eigenstate of the full-quantum Hamiltonian equation (1)–(4). Hence, we are in the bizarre situation that the DNLS apparently describes the experimental results correctly, knowing that we are in a parameter regime where it is *not* valid, while the formally more accurate full-quantum Hamiltonian does not. In light of this discussion, it might seem that the correct result of the DNLS is an *unfortunate coincidence*.

In order to ultimately resolve this issue, Hamm et al. set out to calculate the absorption spectrum of ACN on a numerically exact level [36], along the lines of section 6. In doing so they were guided by the DNLS result that polaron and free exciton may coexist only in 3D, in which case barriers separate both solutions (see section 6), and hence render an exciton solution meta-stable, even if it is slightly higher in energy. This is in accordance with the well known result from a simple quantum mechanical treatment of a square well potential in three dimensions, where a bound state appears only if the product $E_0 a^2$ exceeds a threshold value (with E_0 the depth and a the width of the well). In contrast, an one-dimensional square well has at least one bound state for any value of $E_0 a^2$ [43].

Hamm et al. were furthermore guided by the observation obtained from inspection of the 3D structure of the ACN crystal (figure 1(a)) that exciton coupling along the hydrogen bond direction is negative ($J_\parallel > 0$), while the coupling between hydrogen bond chains is expected to be positive ($J_\perp < 0$). This is since exciton coupling is dominated by through-space transition-dipole coupling [44,45]:

$$J = -\frac{\mu_i \cdot \mu_j}{r_{ij}^3} + 3\frac{(\mu_i \cdot \mathbf{r_{ij}})(\mu_j \cdot \mathbf{r_{ij}})}{r_{ij}^5}, \tag{57}$$
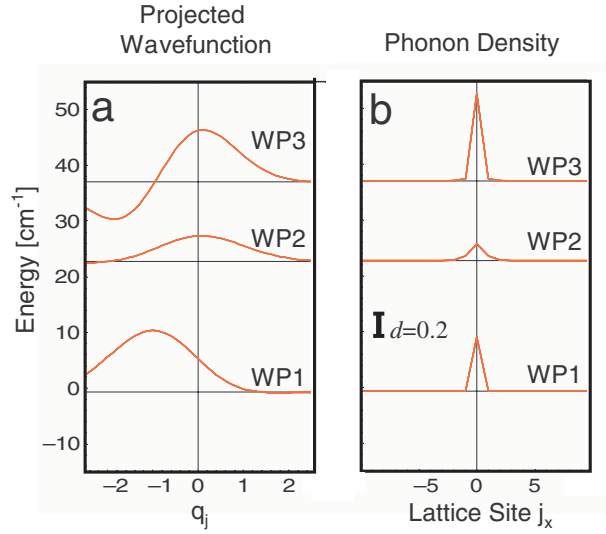
Fig. 12. (a) Projection of (t = 0) wavepackets onto phonon coordinate q and (b) the corresponding phonon-densities $d(j) = \langle \Psi | B_0^\dagger B_0 b_j^\dagger b_j | \Psi \rangle$. Wavepackets WP1, WP2 and WP3 are constructed from the embraced eigenstates as shown in figure 11. The parameters in this simulation were: $\hbar\omega = 50 \, \text{cm}^{-1}$, $\chi = 25 \, \text{cm}^{-1}$, $J_\parallel = 10 \, \text{cm}^{-1}$, $J_\perp = -10 \, \text{cm}^{-1}$. Adapted from [36].

where μ_i and μ_j are the C = O transition dipoles of two sites (as vectors) and $\mathbf{r_{ij}}$ is a vector connecting them. The nearest neighbor distance r_{ij} along the hydrogen-bonded chain is essentially the same as that between chains [46], which is why inter- and intra-chain couplings are expected to be of the same order, albeit with opposite signs. There is no reason to assume that inter-chain coupling can be neglected.

Introducing anisotropy into the exciton coupling increases the parameter space considerably. In [36], an extensive search in parameter space was performed, staying within limits that seemed physically meaningful for the ACN problem, and looking for full-quantum solutions that predict coexistence of free exciton and polaron. Figure 11 shows the best result that could be obtained. The total oscillator strength is distributed over many eigenstates, nevertheless, the oscillator strength clusters in a way that two dominant bands remain when convoluting the stick spectrum with a Lorentzian lineshape function of width $10 \, \text{cm}^{-1}$ (FWHM). The thus obtained spectrum resembles the experimental 30 K spectrum reasonably well (figure 2). The separation of the two bands ($\approx 20 - 30 \, \text{cm}^{-1}$) is somewhat larger than in the experiment, yet it clearly is smaller than one phonon quantum $\hbar\omega$. Furthermore, the higher frequency band shows some substructure in the simulation, similar to the experiment.

We pause and note that we do not observe stationary eigenstates in a femtosecond pump-probe experiment (which are not resolved anyway in reality due to broadening mechanisms). Rather, a femtosecond laser pulse is spectrally broad (due to its shortness) and impulsively excites a coherent superposition state (wavepacket) of all eigenstates that are covered by the spectral width of the pump-pulse. The typical width of the pulses used in [20,21] was $10 \, \text{cm}^{-1}$, which is why it makes sense to discuss the properties of the wavepackets WP1, WP2 and WP3 (as indicated in figure 11), rather than that of individual eigenstates.

A closer analysis shows that the eigenstates that cluster in the lower frequency band (WP1) resemble a ground state harmonic oscillator wavefunction with an origin displacement of about 1 (see figure 12(a)), which is somewhat larger than the value predicted from the simple displaced oscillator picture with $q = \sqrt{2}\chi/\omega \approx 0.71$. The eigenstates that cluster in the higher frequency band, on the other hand, can be classified in the following way: The lower energy portion of these states, clustering as a shoulder in the absorption spectrum (WP2), resembles ground state harmonic oscillator wavefunctions *without any displacement*, while the higher energy portion (WP3) resembles first excited state harmonic oscillator wavefunctions, again *with* origin shift.
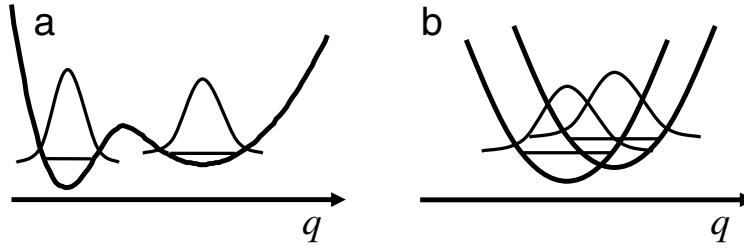
Fig. 13. Two mechanisms that might lead to coexistence of exciton and polaron solutions: (a) two regimes on one effective (adiabatic) potential energy surface separated by a barrier which, however, requires that the length scale of quantum mechanical delocalization of the wavefunction is smaller than that of the barrier, or (b) two effective (adiabatic) surfaces.

Figure 12(b) shows the density of phonons around an exciton, calculated as

$$d(j) = \langle \Psi | B_0^\dagger B_0 b_j^\dagger b_j | \Psi \rangle \tag{58}$$

which reveals essentially the same result: Wavepackets WP1 and WP3 represent phonons dressed around an excitons, i.e. ground and first excited state of a polaron, whereas wavepacket WP2 has much smaller phonon contribution (albeit not zero). Hence, the results seem to be in reasonable agreement with experimental observation. However, it should be noted that such free-exciton like solutions are found only in a very limited parameter regime. In particular, they are found only when exciton couplings with alternating signs of $J_\parallel$ and $J_\perp$ are introduced. The appearance of the double peak structure in the absorption spectrum of crystalline ACN thus seems to depend relatively critically on a balance of parameters, which might explain why vibrational self-trapping is observed so clearly only in ACN, while related crystals show, if at all, only minor effects [22]. It is important to note that equivalent exciton-like solutions could not be found in 1D, where the displaced oscillator picture (section 4.2) remains intact even for relatively large exciton couplings J.

In section 6 we have seen that exciton and polaron solutions may coexist in certain parameter regimes in the 3D case, as a result of a barrier that separates the two regions (figure 5). We find such a barrier only in the regime where the adiabatic DNLS becomes valid, i.e. for $\chi/\hbar\omega \gg 1$, while the transition between exciton and polaron is smooth in the quantum regime (figure 8). This can be rationalized as follows: In the quantum case ($\chi/\hbar\omega < 1$), the potential phonon displacement q is of the order of one or smaller, where the phonon displacement is defined in units of quantum mechanical delocalization length. In other words, quantum-mechanics would average out any barrier that occurs on length scales smaller than the delocalization length of the phonon wavefunction. In that sense, the coexistence of polaron and exciton solutions found in the numerically exact solution of the Holstein Hamiltonian (figure 12) is due to an effect that is different from the one discussed in section 6: It is not a barrier on an effective (adiabatic) ground state surface (figure 13(a)), but must be related to at least two adiabatic surfaces, as sketched in figure 13(b). A physical picture of these two surfaces, apart from the black-box result from the numerically exact diagonalization of the full Hamiltonian, still remains to be developed. Nevertheless, clearly it is the 3D nature of the problem that is responsible for exciton-like solutions. In 1D, the displaced oscillator picture (section 4.2), which does not predict any exciton solutions, remains intact in a wide parameter range.

8 Summary and conclusions

From its first appearance in the literature in 1983, the temperature dependent peak of the C = O vibrations in acetanilide has been associated to the Davydov soliton idea. The latter assumes that when excitons are coupled strongly to acoustic phonons a soliton-like excitation forms that may propagate ballistically. Although Scott and collaborators used optical phonons

for acetanilide, their selftrapping approach was similar to that of Davydov. The Davydov soliton idea has been very appealing from the very beginning since it asserts that nonlinear type modes play an important role in energy transfer in biology. Nonlinearity, of course, is not unknown to biology; on the contrary most functional motions of macromolecules are large amplitude ones and thus nonlinear. The theoretical as well as experimental fascination with acetanilide over a period of more than two decades results fundamentally from its similarity to peptide systems. If soliton-like objects exist in acetanilide then one may investigate their presence and function in proteins.

On the theoretical side, the basic model of Scott for acetanilide involves the following elements: (i) The system is assumed to be one dimensional. This is because the $C = O$ dipoles along the hydrogen-bond axis seem to interact stronger among them than with the ones in the perpendicular directions. (ii) A bear vibrational $C = O$ excitation that tunnels slowly from bond to bond ($J = 5\,cm^{-1}$) couples to a single optical phonon (or to few phonons) of frequency $\omega = 50\,cm^{-1}$ with coupling $\chi = 25\,cm^{-1}$. As a result a localized small polaron of the type of a DNLS discrete breather forms. (iii) The double absorption peak in the amide I region results from the polaron state at $1650\,cm^{-1}$ and the free exciton at $1665\,cm^{-1}$ (iv) The temperature dependence of the polaron state arises from the Frank–Condon factors connecting the unexcited phonon ground state with the displaced phonons in the excited polaron state. This theoretical Scott picture that is adiabatic in nature since it employs the Davydov methodology, was corroborated by Alexander and Krumhansl with the modification that acoustic phonons are also involved.

In order to converge to the polaron picture, numerous alternative explanations had to be eliminated. The most serious objection to the polaron comes for the Fermi-resonance idea, viz. the accidental degeneracy of the amide I symmetric stretch mode with a combination band of an in-plane N-H bend deformation as well as a torsional mode [40]. Although Raman as well as neutron scattering experiments by Barthes and collaborators largely eliminated this possibility, the mere fact that upon complete deuteration the anomalous peak disappears, presents a yet unexplained feature that could speak in favor of a Fermi resonance [17,47]. An alternative issue is related to the active presence of acoustic modes in selftrapping; although there is indication of their absence from incoherent neutron scattering, there is no direct measurement yet of the presumed optical modes that are excited in the processes of the $C = O$ vibrations. While these two experimental issues seem to be still pending all other questions regarding the role of low IR modes, presence of defects or possible hydrogen bond non-degeneracies have been conclusively addressed by the group of Barthes.

While most of the absorption and scattering experiments were done in the eighties and nineties, the recent pump-probe experiments of Hamm and collaborators provide more direct information on the nature of the states involved. Through experiments in the acetanilide N-H band was possible to identify a $50\,cm^{-1}$ hydrogen bond related mode that assists selftrapping in this band. One then makes the natural assumption (compatible with the earlier work) that this phonon is responsible for the amide I selftrapping as well. Furthermore, in pump-probe experiments in the amide I region itself, they found that while the low frequency $1650\,cm^{-1}$ band corresponds indeed to a nonlinear mode, the $1665\,cm^{-1}$ one is certainly a linear one. As result, the former may be assigned to a selftrapped polaron state while the latter to a free exciton one, in a manner compatible with adiabatic theory of Scott.

This adiabatic theoretical polaron scheme has been challenged recently by an exact diagonalization performed on the Holstein Hamiltonian as applied to the specific acetanilide problem. Using a numerically exact procedure Hamm et al. found that while the polaron state could be identified as the lowest energy state, the free exciton state did not appear in the calculated spectrum [36]. These numerics showed that there is no free exciton state neither in one nor in three dimensions for the "standard" acetanilide parameter values with hopping rate in the range $J \approx 5$–$10\,cm^{-1}$. In order to bypass this problem, Hamm et al. introduced different signs in the hopping rares depending on direction, viz. negative overall rates along the hydrogen-bonded axis while positive along the plane perpendicular to it. The resulting spectrum is then compatible with the experiment within the standard parameter regime.

The issue of the free exciton state has been discussed extensively in the present work. Using the semiclassical theory of Kalosakas et al., we showed that in three dimensions free exciton and polaron states are separated by a barrier while there is no such barrier in one dimension [27]. Furthermore, for the standard acetanilide parameter regime the one dimensional semiclassical free exciton state has quite a short lifetime and is in general unstable. Thus, even semiclassically, the one-dimensional acetanilide picture needs to be revised. Using the double well adiabatic potential for free exciton and polaron and upon an ad-hoc requantization we find that the resulting two lowest states have polaron and free-exciton features respectively. Thus, within this intuitive, yet approximate, 3D picture we recapture in principle Scott's original explanation. The problem is that this result does not appear to agree quantitatively with the exact numerics mentioned above, unless different sign hopping terms are used in the latter.

Cristaline acetanilide proved to be a good medium for experiment as well as theory for over twenty five years. During this period it permit the application of diverse experimental techniques as well as the testing of a large variety of theoretical ideas. It is clear that although many issues have been addressed and resolved, there are still many challenges ahead. In addition to the central dimensionality issue related to the free exciton, the absence of a temperature dependent peak from the fully deuterated acetanilide or the dispersion features of the modes that assist selftrapping need to be understood better. Furthermore, selftrapping in the N-H bond needs also to be addressed that is actually different compared to that in the $C = O$ bonds. Specifically, while a phonon progression that is absent in the later is seen in the former, it nevertheless terminates abruptly in a way dissimilar to what is expected from equation (31). And while the $C = O$ overtones where treated by Scott through QDNLS, it would be interesting to analyze them directly through the Holstein model. It is clear that the exciting "acetanilide story" is far from over.

9 Appendix: Brief historical guide to the research in ACN

Due to the numerous number of works published on the "Davydov soliton" as well as ACN, it is often hard to keep track of the various contributions and the significant developments in the "acetanilide story". We present here a partial list of contributions in a historical order that are specifically relevant to the acetanilide developments.

- 1973 Davydov introduces the idea that as a result to coupling with acoustic phonons a vibrational excitation may selftrap and become a non-topological soliton [3]. Careri finds experimentally an "anomalous peak" in acetanilide [6].
- 1982 Davydov publishes his book on "Biology and Quantum Mechanics" where he details his approach to energy transfer in biomolecules [23].
- 1983 Careri, Scott and collaborators present experimental and theoretical analysis of the $C = O$ band of crystalline acetanilide [7]. After eliminating possible alternative explanations they conclude that the temperature dependent ACN peak at $1650\,\text{cm}^{-1}$ is due to a "Davydov soliton" type mechanism.
- 1984 Careri, Scott and collaborators present detailed experimental and theoretical details on the acetanilide "anomalous peak" [8]. Eilbeck, Lomdahl and Scott analyze selftrapping of the amide I mode through the Discrete Selftrapping equation [9].
- 1985 Alexander treats theoretically the Davydov Hamiltonian using Holstein polaron techniques [13]. Blanchet and Fincher find experimentally that low IR as well as a band at $3250\,\text{cm}^{-1}$ have the same temperature dependence as that of the "anomalous peak" and suggest that a topological defect might be responsible for the anomalous amide structure [39].

Johnston and Swanson propose that that the anomalous peak is a result of Fermi resonance between the amide I mode and a combination mode between an N-H motion and a strongly temperature dependent low frequency phonon [40]. Scott and collaborators introduce the quantum DST equation and explain higher frequency anomalous lines as overtone spectra of the C = O band [41].

- 1986 Takeno introduces a classical vibron model and studies the acetanilide temperature dependence in a way similar to that of localized modes in alkali halides [48]. Alexander and Krumhansl provide an adiabatic treatment of the Davydov Hamiltonian and analyze the ACN peak using an acoustic phonon chain [14].
- 1988 Barthes and coworkers study experimentally acetanilide and while confirm the presence of anharmonicity in the solid they report no evidence of acoustic phonons involved in selftrapping [24].
- 1989 Scott uses the theory of color centers and proposes a quantitative explanation for the temperature dependence of the "anomalous" ACN peak [15].
- 1990 Austin and collaborators perform pump-probe experiments in acetanilide and propose that the temperature dependence of the anomalous peak is due to hydrogen bond non-degeneracy [29].
- 1991 Barthes and collaborators show through inelastic neutron scattering experiments that ACN data are not consistent with a topological defect assumption [17]. They also claim that no indication of acoustic phonons are seen in the low IR spectra. Furthermore through Raman scattering experiments they report that while fully deuterated acetanilide shows no anomalous peak, a partially deuterated one does have one, downshifted however by about $150\,cm^{-1}$ from the main amide I peak.
- 1992 Scott summarizes the "Davydov soliton" and the "acetanilide story" in a review article in Physics Reports [10].
- 1995 Barthes and collaborators use neutron scattering experiments and find no non-degeneracy in the hydrogen-bonded proton [30].
- 1999 Kalosakas, Aubry and Tsironis investigate the semiclassical Holstein model and propose that phononic normal modes of the semiclassical polaron may be related to low frequency ACN modes [27,49].
- 2000 Barthes and collaborators show that the low IR modes investigated earlier have no anomalous temperature dependence [50].
- 2002 Hamm, Edler and Scott use pump-probe experiments and analyze the NH spectrum of ACN [19]. They identify a phonon of approximately $50\,cm^{-1}$ that seems to be involved in selftrapping of the exciton. Hamm and Edler publish pump-probe experiments for the C = O band that identify the "anomalous" peak as a nonlinear state and the "normal" one as a linear free exciton state [20].
- 2006 Hamm and collaborator present a numerical diagonalization of the Holstein model in one and three dimensions and find inconsistencies between numerical results in one dimension and standard adiabatic anomalous peak explanation. They propose that the C = O polaron are a result of the three dimensional nature of the ACN crystal as well as specific exciton dipole-dipole matrix elements [36].

References

1. For historical and other details on solitons consult [2]
2. T. Dauxois, M. Peyrard, *Physics of Solitons* (Cambridge University Press, 2006)
3. A.S. Davydov, N.I. Kislukha, Phys. Stat. Sol. **59**, 465 (1973)
4. A.S. Davydov, J. Theor. Biol. **66**, 379 (1977)
5. A.S. Davydov, Phys. Scr. **20**, 387 (1979)
6. G. Careri, *Cooperative Phenomena*, edited by H. Haken, M. Wagner (Springer, Berlin, 1973)
7. G. Careri, U. Buontempo, F. Carta, E. Gratton, A.C. Scott, Phys. Rev. Lett. **51**, 304 (1983)
8. G. Careri, U. Buontempo, F. Galluzzi, A.C. Scott, E. Gratton, E. Shyamsunder, Phys. Rev. B **30**, 4689 (1984)
9. J.C. Eilbeck, P.S. Lomdahl, A.C. Scott, Phys. Rev. B **30**, 4703 (1984)

10. A.C. Scott, Phys. Rep. **217**, 1 (1992)
11. D.W. Brown, K. Lindenberg, B.J. West, Phys. Rev. A **33**, 4104 (1986)
12. D.W. Brown, K. Lindenberg, B.J. West, Phys. Rev. A **33**, 4110 (1986)
13. D.M. Alexander, Phys. Rev. Lett. **54**, 138 (1985)
14. D.M. Alexander, J.A. Krumhansl, Phys. Rev. B **33**, 7172 (1986)
15. A.C. Scott, I.J. Bigio, C.T. Johnston, Phys. Rev. B **39**, 12883 (1989)
16. M. Barthes, J. Mol. Liq. **41**, 143 (1989)
17. M. Barthes, R. Almairac, J.L. Sauvajol, J. Moret, R. Currat, J. Dianoux, Phys. Rev. B **43**, 5223 (1991)
18. A. Sievers, S. Takeno, Phys. Rev. Lett. **61**, 1988 (1988)
19. J. Edler, P. Hamm, A.C. Scott, Phys. Rev. Lett. **88**, 067403 (2002)
20. J. Edler, P. Hamm, J. Chem. Phys. **117**, 2415 (2002)
21. J. Edler, P. Hamm, J. Chem. Phys. **119**, 2709 (2003)
22. J. Edler, P. Hamm, Phys. Rev. B **69**, 214301 (2004)
23. A.S. Davydov, *Biology and Quantum Mechanics* (Pergamon, New York, 1982)
24. M. Barthes, R. Almairac, J.L. Sauvajol, R. Currat, J. Moret, J.L. Ribet, Europhys. Lett. **7**, 55 (1988)
25. D.B. Fitchen, *Physics of Color Centers*, edited by W.B. Fouler (Academic Press, New York, 1968) pp. 293–350
26. T. Holstein, Ann. Phys. **8**, 325 (1959)
27. G. Kalosakas, S. Aubry, G.P. Tsironis, Phys. Rev. B **58**, 3094 (1998)
28. J.C. Eilbeck, P.S. Lomdahl, A.C. Scott, Physica D **16**, 318 (1985)
29. W. Fann, L. Rothberg, M. Roberson, S. Benson, J. Madey, S. Etemad, R. Austin, Phys. Rev. Lett. **64**, 607 (1990)
30. S.W. Johnson, M. Barthes, J. Eckert, R.K. McMullan, M. Muller, Phys. Rev. Lett. **74**, 2844 (1995)
31. D.W. Brown, Z. Ivić, Phys. Rev. B **40**, 9876 (1989)
32. S. Aubry, in *Polarons in Advanced Materials*, edited by A.S. Alexandrov (Canopus/Springer Publishing, 2007), p. 315
33. I.G. Lang, Y.A. Firsov, Sov. Phys. JETP **16**, 1301 (1963)
34. T. Holstein, Ann. Phys. **343-389**, 325 (1959)
35. A.C. Scott, J.C. Eilbeck, H. Gilhøj, Physica D **78**, 194 (1994)
36. P. Hamm, J. Edler, Phys. Rev. B **73**, 094302 (2006)
37. J. Bonča, S.A. Trugman, I. Bastistić, Phys. Rev. B **60**, 1633 (1999)
38. L.C. Ku, S.A. Trugman, J. Bonča, Phys. Rev. B **65**, 174306 (2001)
39. G.B. Blanchet, C.R. Fincher, Phys. Rev. Lett. **54**, 1310 (1985)
40. C.T. Johnston, B.I. Swanson, Chem. Phys. Lett. **114**, 547 (1985)
41. A.C. Scott, E. Gratton, E. Shyamsunder, G. Careri, Phys. Rev. B **32**, 5551 (1985)
42. H. Feddersen, Phys. Lett. A **154**, 391 (1991)
43. L. Schiff, *Quantum Mechanics* (McGraw-Hill, New York, 1959)
44. S. Krimm, J. Bandekar, Adv. Protein Chem. **38**, 181 (1986)
45. H. Torii, M. Tasumi, J. Chem. Phys. **96**, 3379 (1992)
46. C.J. Brown, D.E.C. Corbridge, Acta Cryst. **7**, 711 (1954)
47. M. Barthes, J. Eckert, S.W. Johnson, J. Moret, B.I. Swanson, C.J. Unkefer, J. Phys. I (France) **2**, 1929 (1992)
48. S. Takeno, Prog. Theor. Phys. **75**, 1 (1986)
49. G. Kalosakas, S. Aubry, G.P. Tsironis, Phys. Lett. A **247**, 413 (1998)
50. A. Spire, M. Barthes, H. Kellouai, G.D. Nunzio, Physica D **137**, 392 (2000)